Supporting information for:
Design, Synthesis, and Study of Lactam and Ring-Expanded Analogues of Teixobactin

Hyunjun Yang, Arthur V. Pishenko, Xingyue Li, and James S. Nowick*

Department of Chemistry, University of California, Irvine,
Irvine, California 92697-2025, United States

Email: jsnowick@uci.edu

Table of contents

Supplemental Text, Figures, and Table

On-resin Synthesis of D-Aza-Threonine. We developed conditions for the on-resin synthesis of D-aza-threonine from D-*allo*-threonine in a model system comprising an Ala-D-aza-Thr-Gln tripeptide. Initial efforts to convert D-*allo*-Thr to the corresponding mesylate and then to the azide on resin with inversion of stereochemistry resulted in elimination to the dehydroamino acid as the predominant product (Figure S1). We found that the elimination reaction could be avoided by introducing the azide group before elongating the peptide chain (Figure S2). As the Fmoc protecting group is labile to azide, the Fmoc group on D-*allo*-Thr is first replaced with an Alloc protecting group (Figure S3). The resin-bound Alloc-D-*allo*-Thr-Gln(Trt) dipeptide is converted to the corresponding mesylate by treatment with triethylamine and mesyl chloride in dichloromethane (Figure S4). The mesylate is converted to the azide with inversion of stereochemistry by treatment with sodium azide in a mixture of 15-crown-5 and DMF at 55 ºC (Figure S5). Alloc deprotection with $(Ph_3P)_4Pd$ and $PhSiH_3$ liberated the α-amino group of D-azido-threonine (Figure S6). Coupling of Boc-Ala-OH with HCTU and 20% collidine in DMF afforded the corresponding tripeptide (Figure S7). Reduction of the azide group with triphenylphosphine-2-carboxamide generated the amino group (Figure S8). Coupling of Fmoc-Ile-OH with HCTU and 20% collidine in DMF introduced Ile on the sidechain of D-aza-Thr (Figure S9). Each of these reactions proceeded smoothly, as indicated by HPLC analysis of small aliquots of peptide cleaved from the resin with 20% hexafluoroisopropanol (HFIP) in CH_2Cl_2 (Figures S3–S9). Collectively, this series of reactions lays the groundwork for the solid-phase peptide synthesis of aza-teixobactin derivatives.

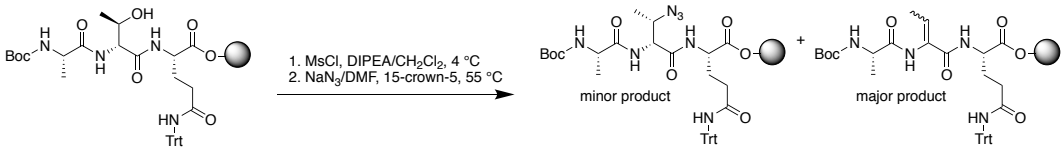

Figure S1. Attempted conversion of resin-bound Boc-Ala-D-*allo*-Thr-Gln(Trt) to Boc-Ala-D-azido-Thr-Gln(Trt) results in elimination to the dehydropeptide.

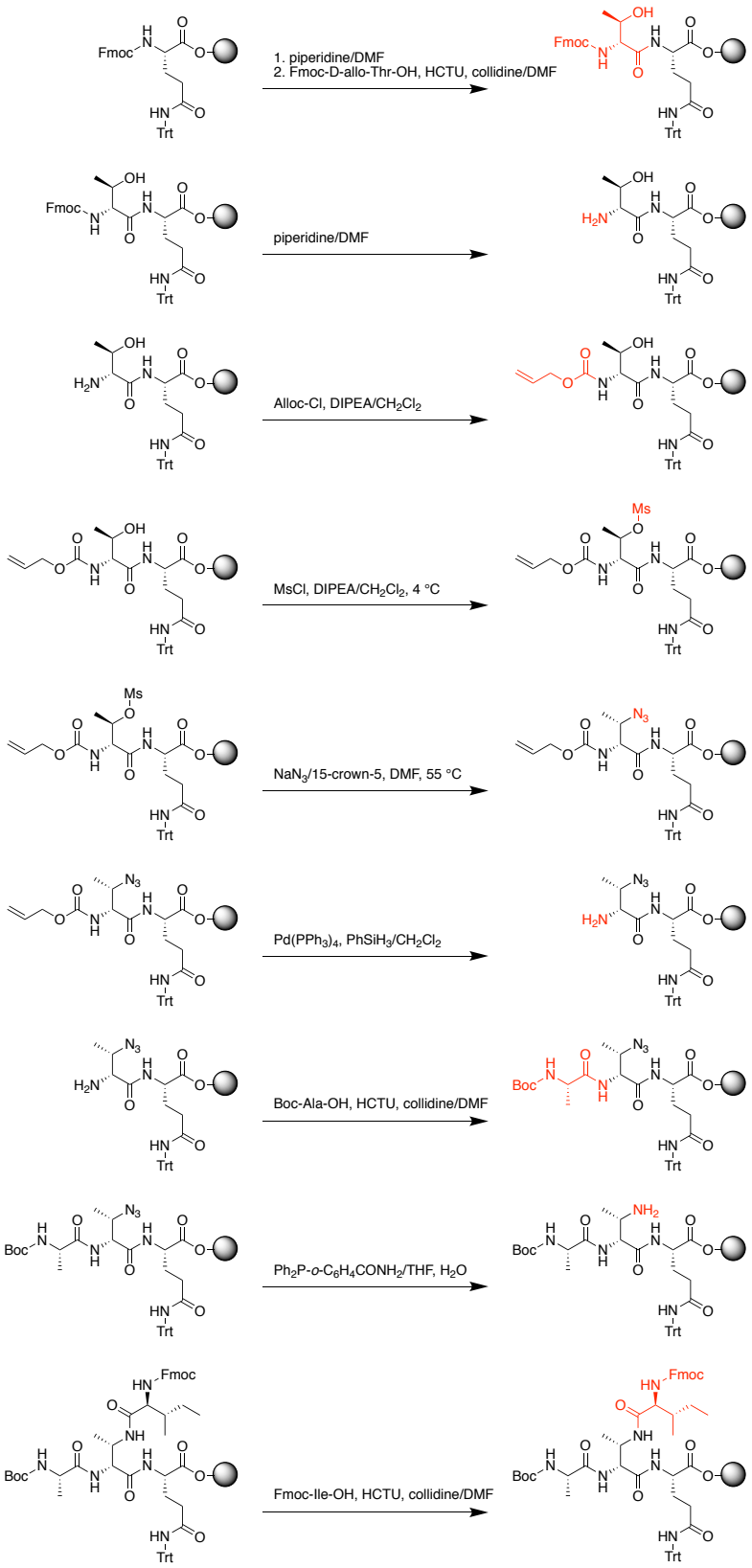

Figure S2. Solid-phase synthesis of a peptide model system containing D-aza-threonine.

Figures S3–S9. HPLC analyses of crude products (Conversion of D-*allo*-threonine to D-aza-threonine).

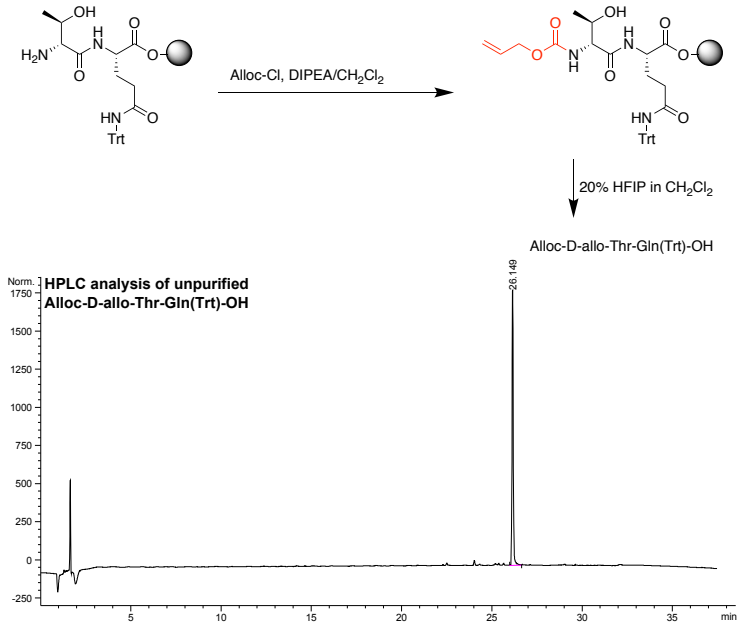

Figure S3. Analytical HPLC trace of Alloc-D-*allo*-Thr-Gln(Trt)-OH. Analytical RP-HPLC was performed on a C18 column with an elution gradient of 5-100% CH_3CN over 30 min.

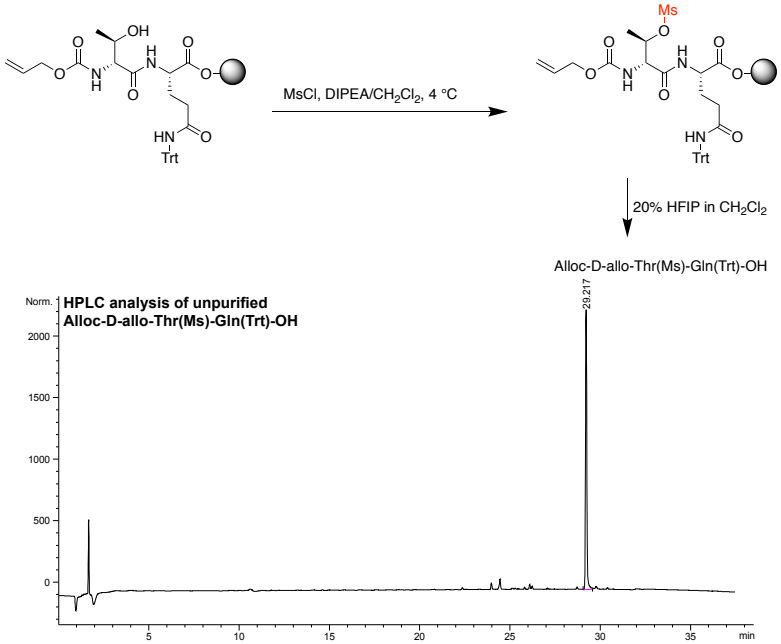

Figure S4. Analytical HPLC trace of Alloc-D-*allo*-Thr(Ms)-Gln(Trt)-OH. Analytical RP-HPLC was performed on a C18 column with an elution gradient of 5-100% CH_3CN over 30 min.

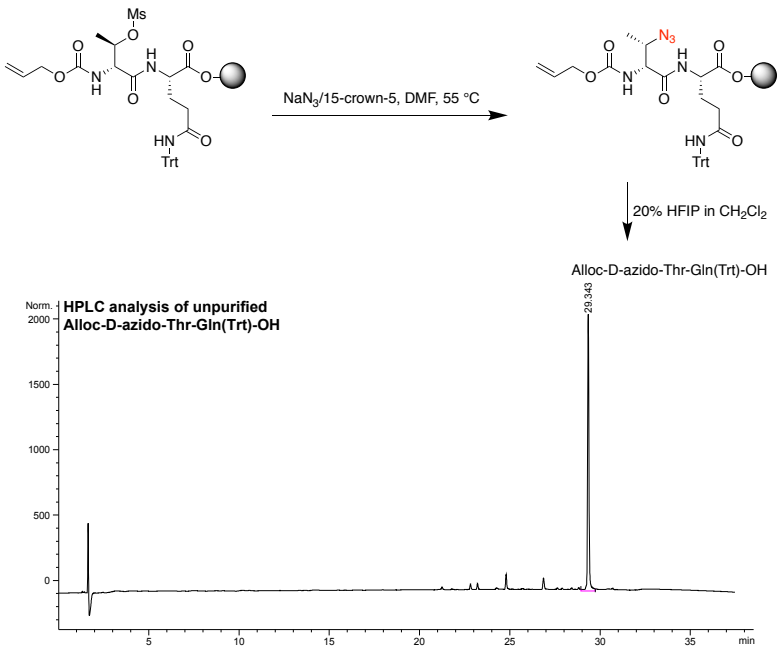

Figure S5. Analytical HPLC trace of Alloc-D-azido-Thr-Gln(Trt)-OH. Analytical RP-HPLC was performed on a C18 column with an elution gradient of 5-100% CH_3CN over 30 min.

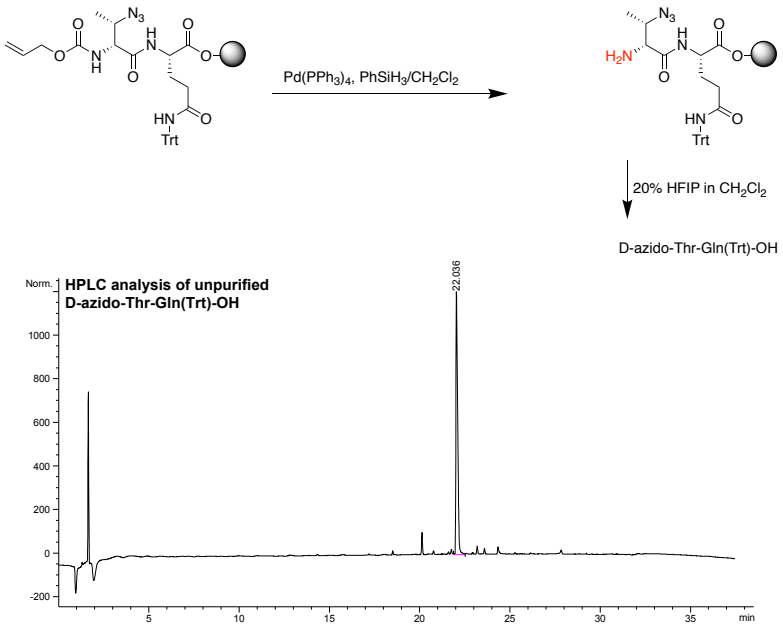

Figure S6. Analytical HPLC trace of D-azido-Thr-Gln(Trt)-OH. Analytical RP-HPLC was performed on a C18 column with an elution gradient of 5-100% CH_3CN over 30 min.

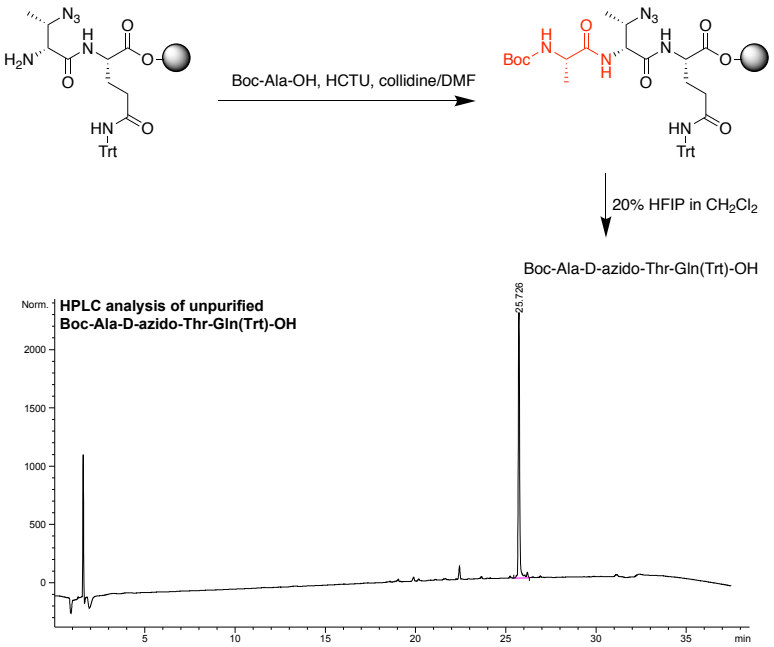

Figure S7. Analytical HPLC trace of Boc-Ala-D-azido-Thr-Gln(Trt)-OH. Analytical RP-HPLC was performed on a C18 column with an elution gradient of 5-100% CH_3CN over 30 min.

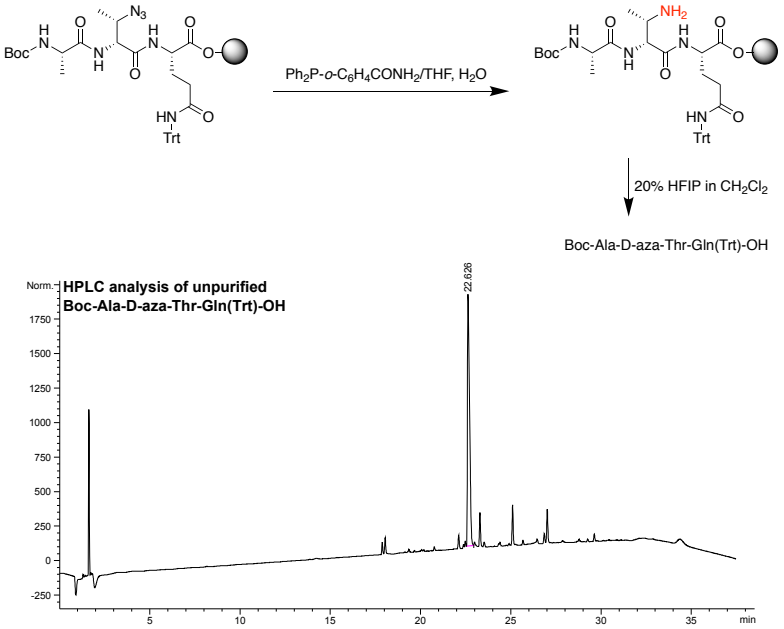

Figure S8. Analytical HPLC trace of Boc-Ala-D-aza-Thr-Gln(Trt)-OH. Analytical RP-HPLC was performed on a C18 column with an elution gradient of 5-100% CH_3CN over 30 min.

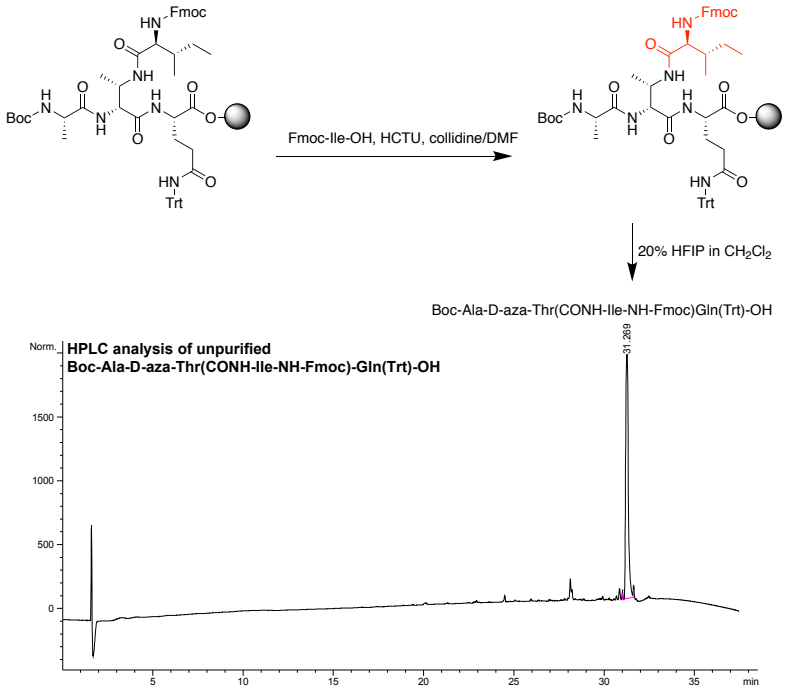

Figure S9. Analytical HPLC trace of Boc-Ala-D-aza-Thr(CONH-Ile-NH-Fmoc-Gln(Trt)-OH. Analytical RP-HPLC was performed on a C18 column with an elution gradient of 5-100% CH_3CN over 30 min.

On-resin Synthesis of Aza-Threonine Stereoisomers. The synthetic route shown above allows the preparation of peptides containing all four stereoisomers of aza-threonine: D-aza-Thr, D-*allo*-aza-Thr, L-aza-Thr, and L-*allo*-aza-Thr. Figures S10-S16 illustrate the synthesis of the model system comprising an Ala-D-aza-*allo*-Thr-Gln tripeptide. Figures S17-S23 illustrate the synthesis of the model system comprising an Ala-L-aza-Thr-Gln tripeptide. Figures S24-S30 illustrate the synthesis of the model system comprising an Ala-L-aza-*allo*-Thr-Gln tripeptide. The reduction of L-*allo*-azido-threonine with triphenylphosphine-2-carboxamide proceeds more slowly than that of the other diastereomers in the Boc-Ala-L-*allo*-azido-Thr-Gln(Trt) model system, but the reaction can be driven to completion by prolonged reaction time (48 h).

Figures S10–S16. HPLC analyses of crude products (Conversion of D-threonine to D-*allo*-aza-threonine).

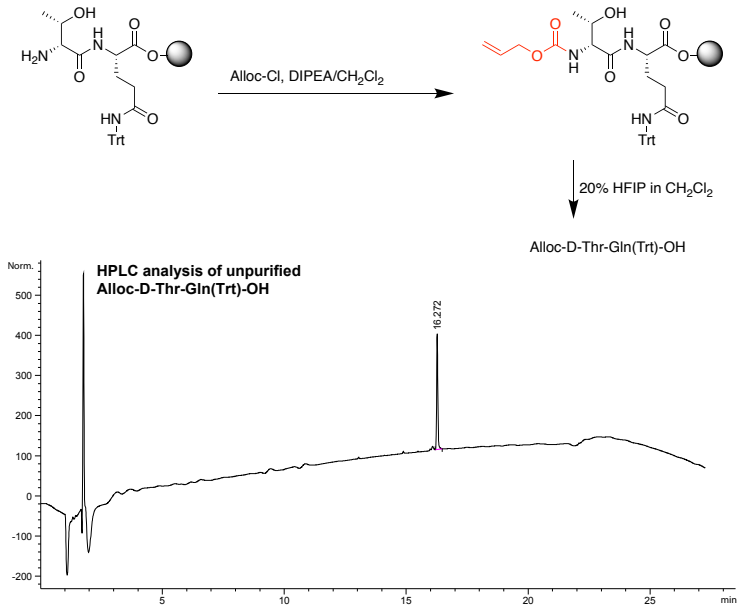

Figure S10. Analytical HPLC trace of Alloc-D-Thr-Gln(Trt)-OH. Analytical RP-HPLC was performed on a C18 column with an elution gradient of 5-100% CH_3CN over 20 min.

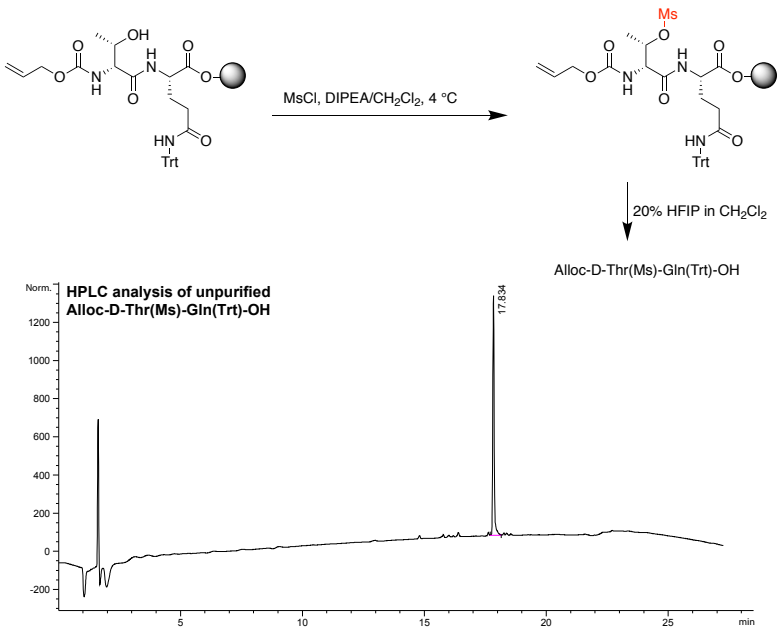

Figure S11. Analytical HPLC trace of Alloc-D-Thr(Ms)-Gln(Trt)-OH. Analytical RP-HPLC was performed on a C18 column with an elution gradient of 5-100% CH_3CN over 20 min.

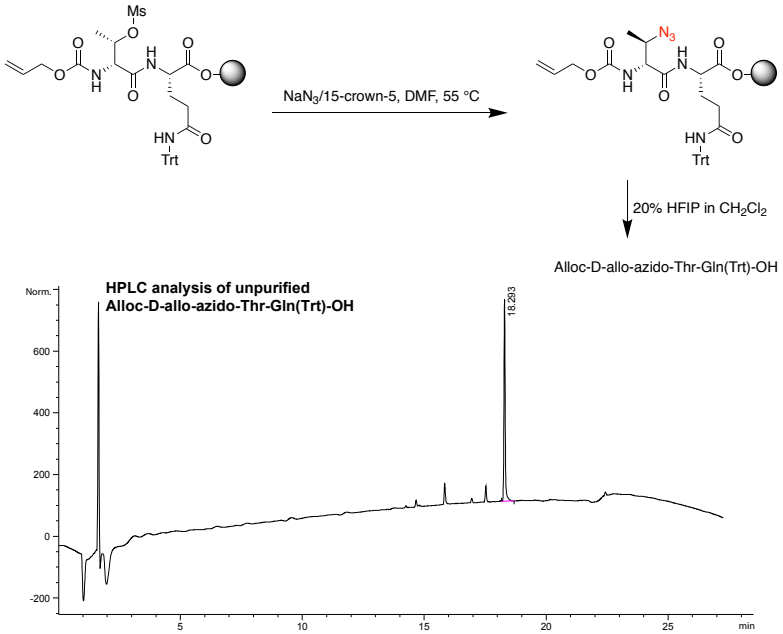

Figure S12. Analytical HPLC trace of Alloc-D-*allo*-azido-Thr-Gln(Trt)-OH. Analytical RP-HPLC was performed on a C18 column with an elution gradient of 5-100% CH_3CN over 20 min.

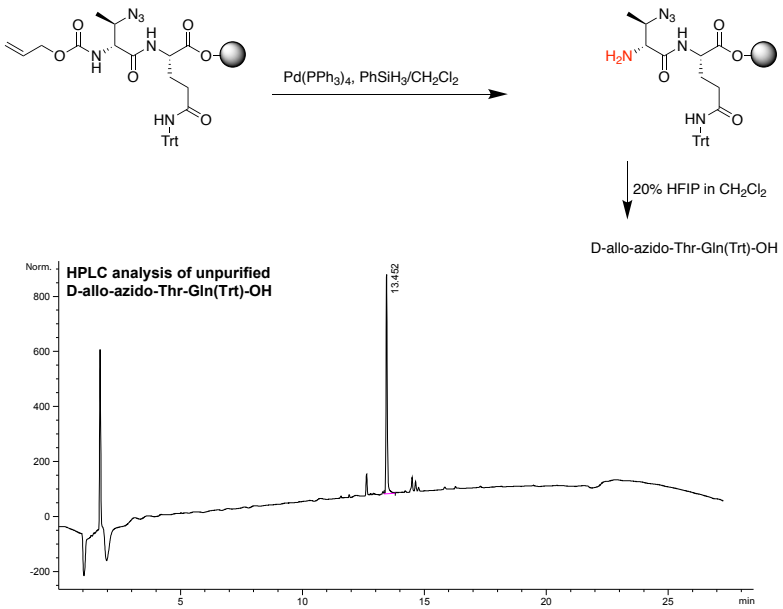

Figure S13. Analytical HPLC trace of D-*allo*-azido-Thr-Gln(Trt)-OH. Analytical RP-HPLC was performed on a C18 column with an elution gradient of 5-100% CH_3CN over 20 min.

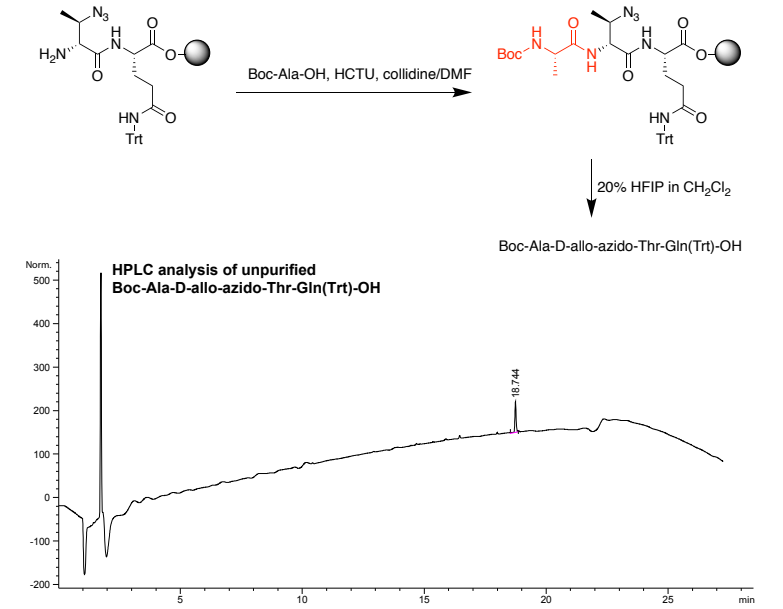

Figure S14. Analytical HPLC trace of Boc-Ala-D-*allo*-azido-Thr-Gln(Trt)-OH. Analytical RP-HPLC was performed on a C18 column with an elution gradient of 5-100% CH_3CN over 20 min.

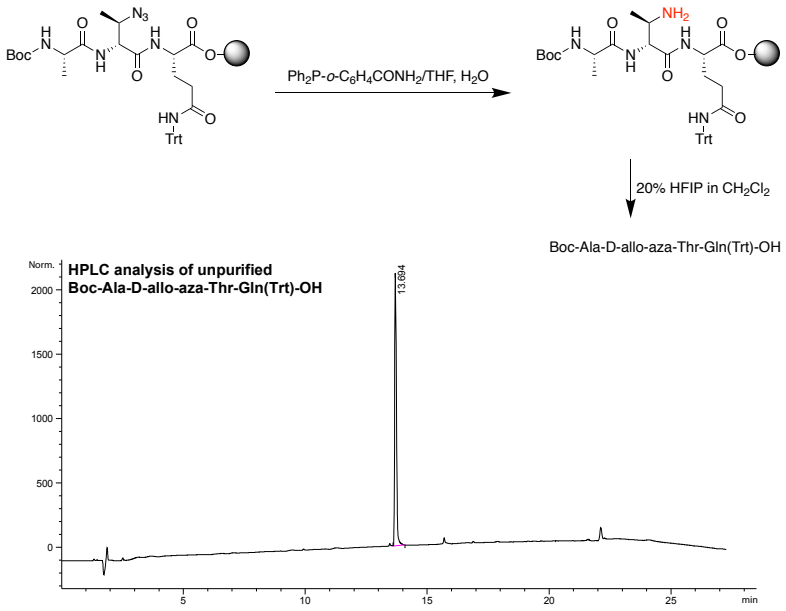

Figure S15. Analytical HPLC trace of Boc-Ala-D-*allo*-aza-Thr-Gln(Trt)-OH. Analytical RP-HPLC was performed on a C18 column with an elution gradient of 5-100% CH_3CN over 20 min.

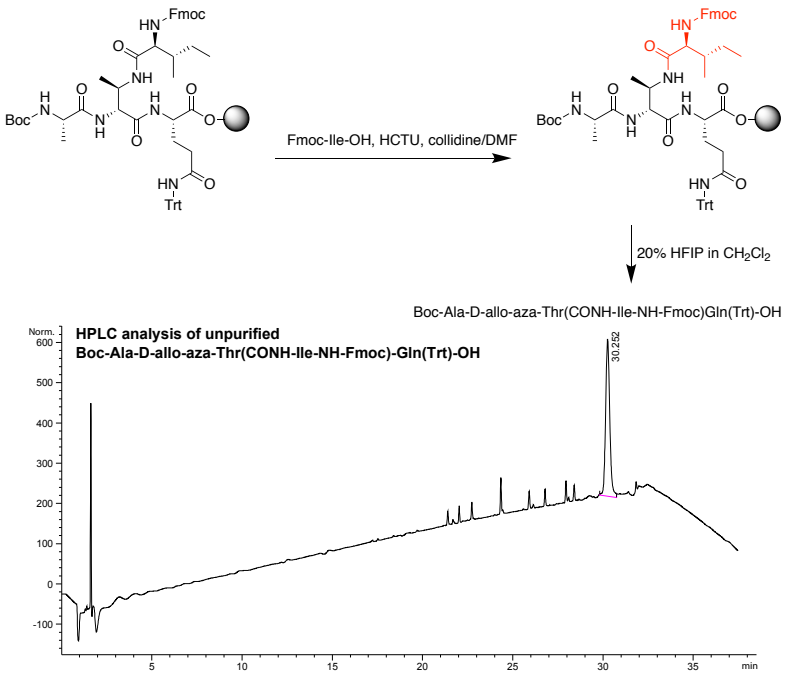

Figure S16. Analytical HPLC trace of Boc-Ala-D-*allo*-aza-Thr(CONH-Ile-NH-Fmoc-Gln(Trt)-OH. Analytical RP-HPLC was performed on a C18 column with an elution gradient of 5-100% CH_3CN over 30 min.

Figures S17–S23. HPLC analyses of crude products (Conversion of L-*allo*-threonine to L-aza-threonine).

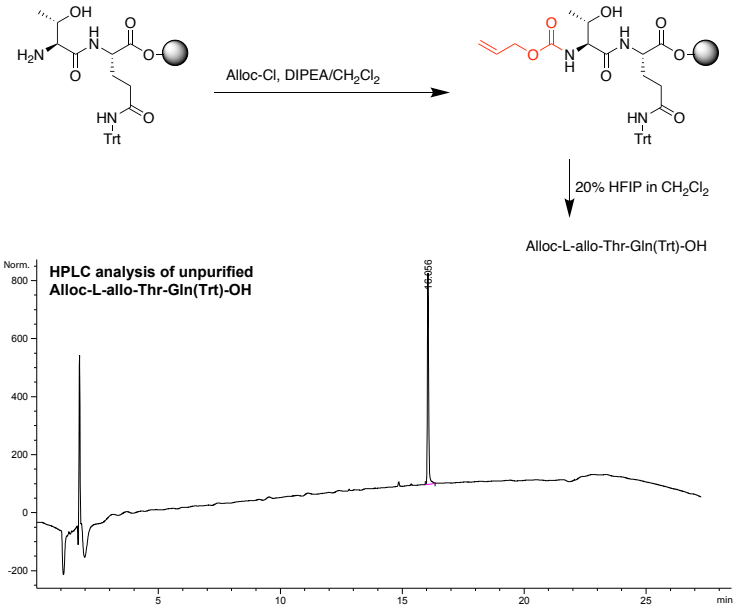

Figure S17. Analytical HPLC trace of Alloc-L-*allo*-Thr-Gln(Trt)-OH. Analytical RP-HPLC was performed on a C18 column with an elution gradient of 5-100% CH_3CN over 20 min.

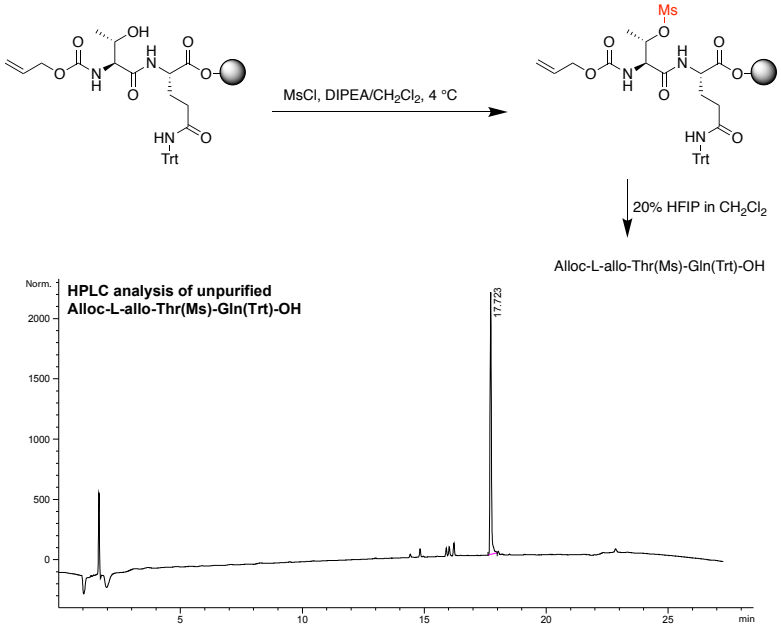

Figure S18. Analytical HPLC trace of Alloc-L-*allo*-Thr(Ms)-Gln(Trt)-OH. Analytical RP-HPLC was performed on a C18 column with an elution gradient of 5-100% CH_3CN over 20 min.

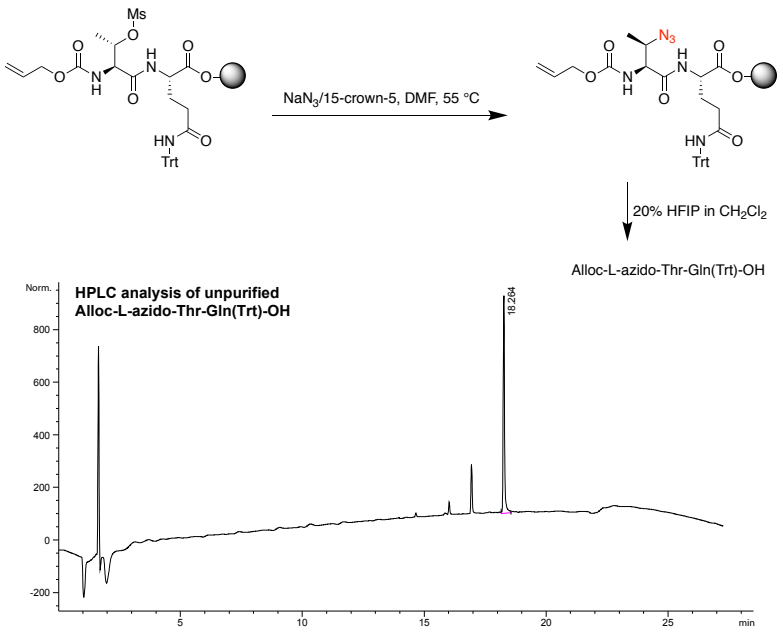

Figure S19. Analytical HPLC trace of Alloc-L-azido-Thr-Gln(Trt)-OH. Analytical RP-HPLC was performed on a C18 column with an elution gradient of 5-100% CH_3CN over 20 min.

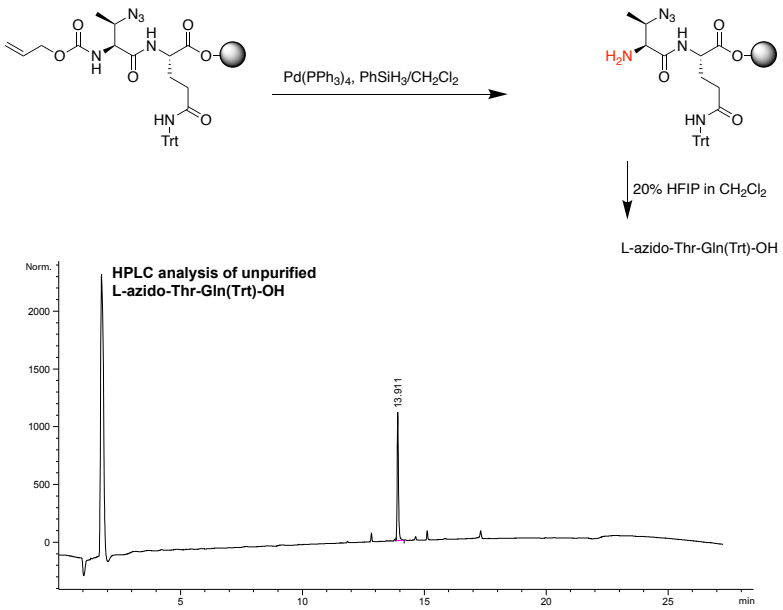

Figure S20. Analytical HPLC trace of L-azido-Thr-Gln(Trt)-OH. Analytical RP-HPLC was performed on a C18 column with an elution gradient of 5-100% CH_3CN over 20 min.

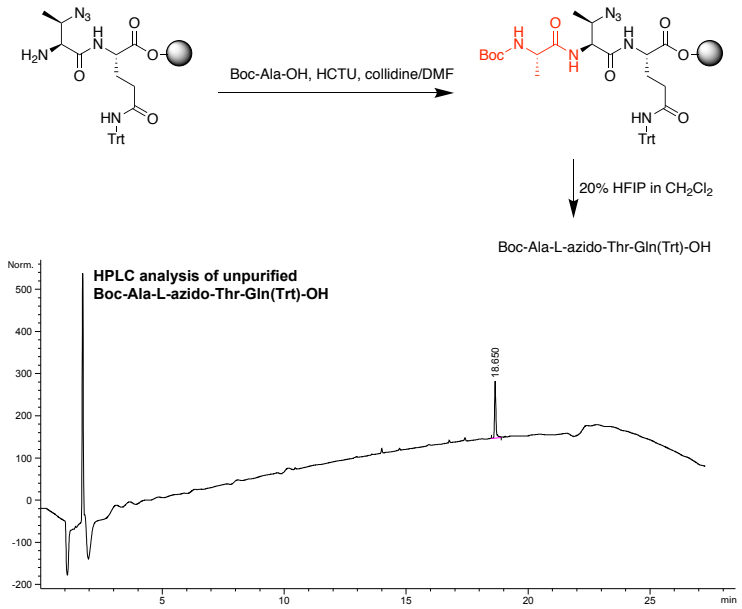

Figure S21. Analytical HPLC trace of Boc-Ala-L-azido-Thr-Gln(Trt)-OH. Analytical RP-HPLC was performed on a C18 column with an elution gradient of 5-100% CH_3CN over 20 min.

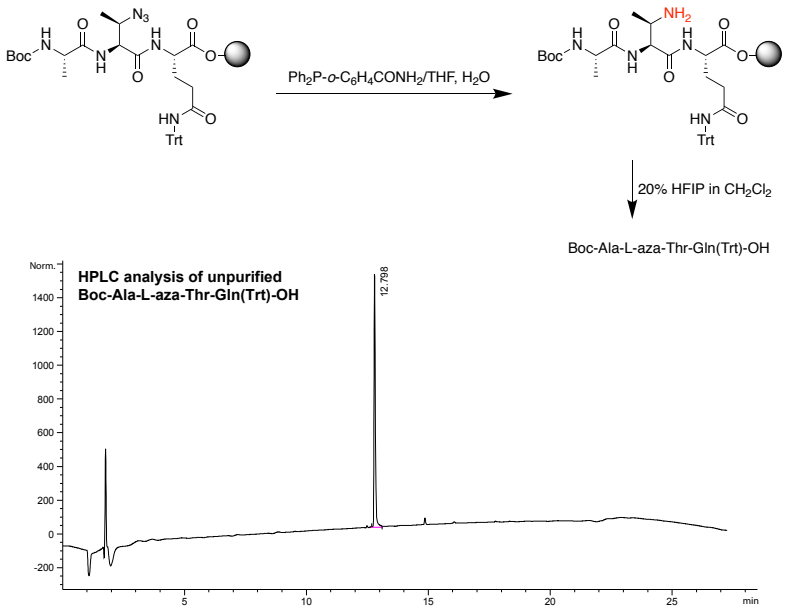

Figure S22. Analytical HPLC trace of Boc-Ala-L-aza-Thr-Gln(Trt)-OH. Analytical RP-HPLC was performed on a C18 column with an elution gradient of 5-100% CH_3CN over 20 min.

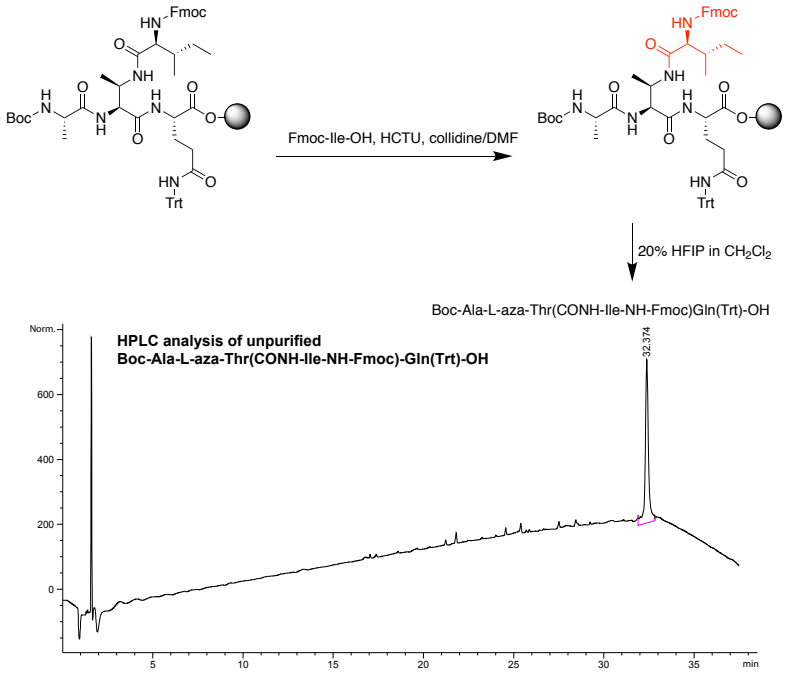

Figure S23. Analytical HPLC trace of Boc-Ala-L-aza-Thr(CONH-Ile-NH-Fmoc-Gln(Trt)-OH. Analytical RP-HPLC was performed on a C18 column with an elution gradient of 5-100% CH_3CN over 30 min.

Figures S24–S30. HPLC analyses of crude products (Conversion of L-threonine to L-*allo*-aza-threonine).

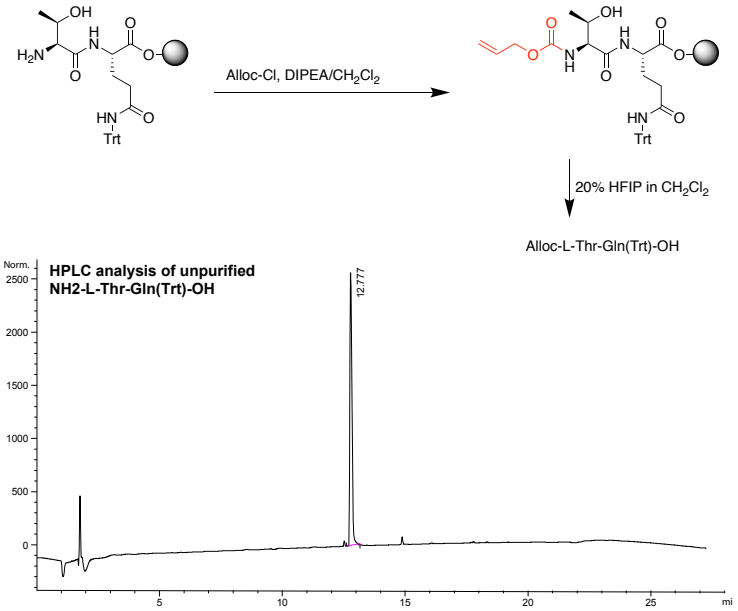

Figure S24. Analytical HPLC trace of Alloc-L-Thr-Gln(Trt)-OH. Analytical RP-HPLC was performed on a C18 column with an elution gradient of 5-100% CH_3CN over 20 min.

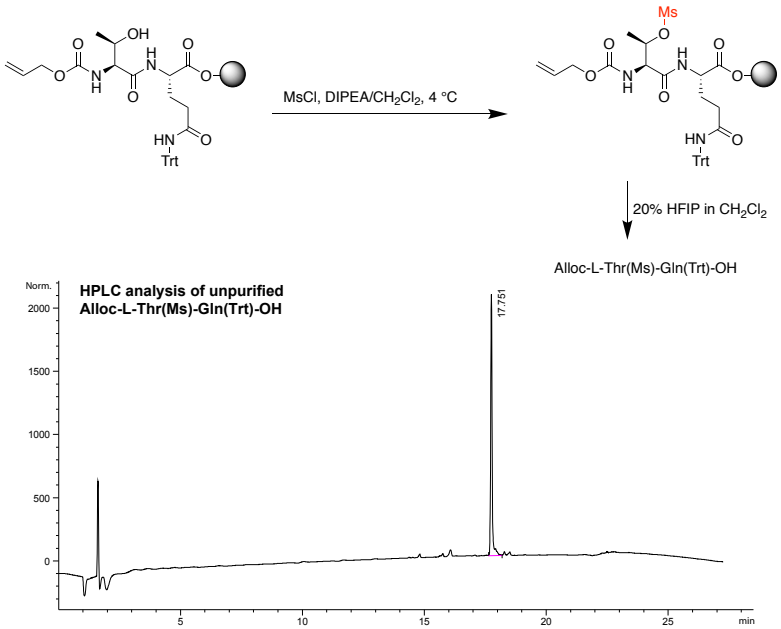

Figure S25. Analytical HPLC trace of Alloc-L-Thr(Ms)-Gln(Trt)-OH. Analytical RP-HPLC was performed on a C18 column with an elution gradient of 5-100% CH_3CN over 20 min.

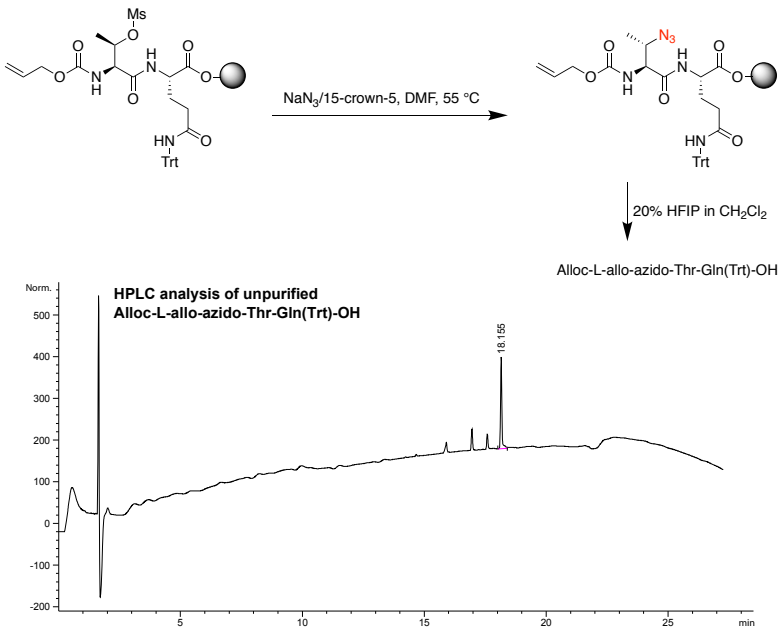

Figure S26. Analytical HPLC trace of Alloc-L-*allo*-azido-Thr-Gln(Trt)-OH. Analytical RP-HPLC was performed on a C18 column with an elution gradient of 5-100% CH_3CN over 20 min.

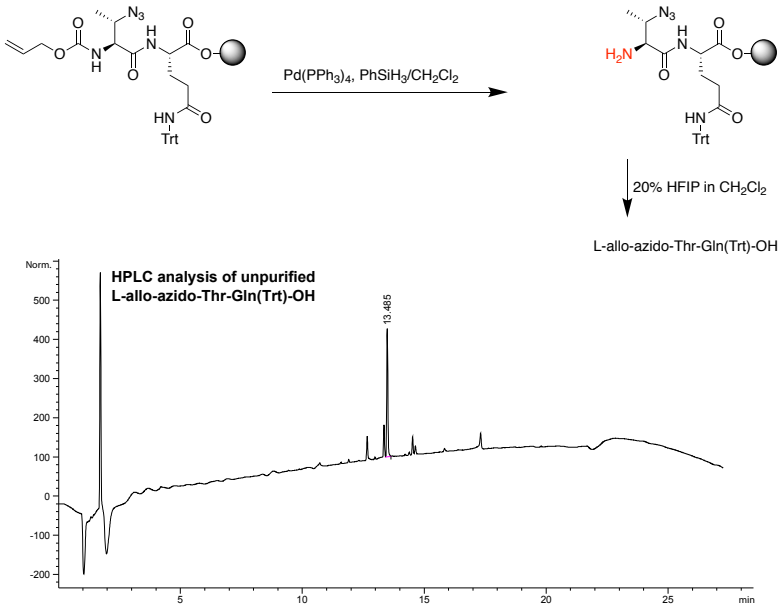

Figure S27. Analytical HPLC trace of L-*allo*-azido-Thr-Gln(Trt)-OH. Analytical RP-HPLC was performed on a C18 column with an elution gradient of 5-100% CH_3CN over 20 min.

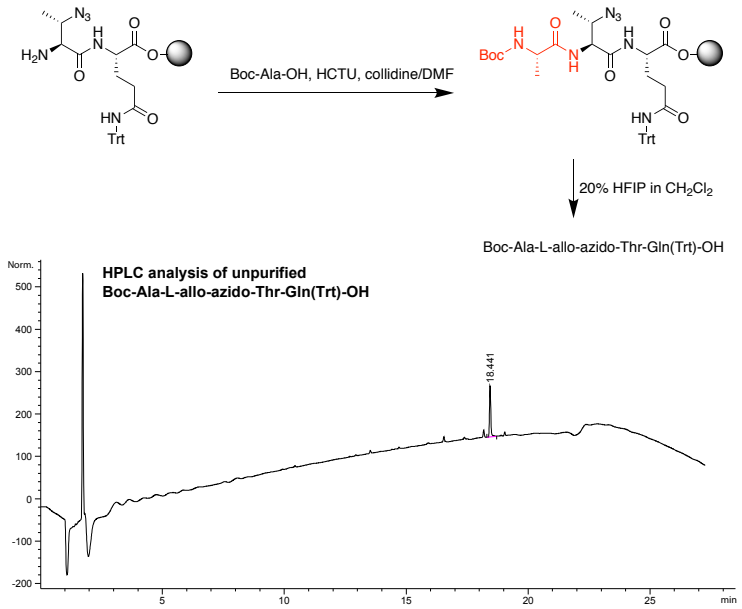

Figure S28. Analytical HPLC trace of Boc-Ala-L-*allo*-azido-Thr-Gln(Trt)-OH. Analytical RP-HPLC was performed on a C18 column with an elution gradient of 5-100% CH_3CN over 20 min.

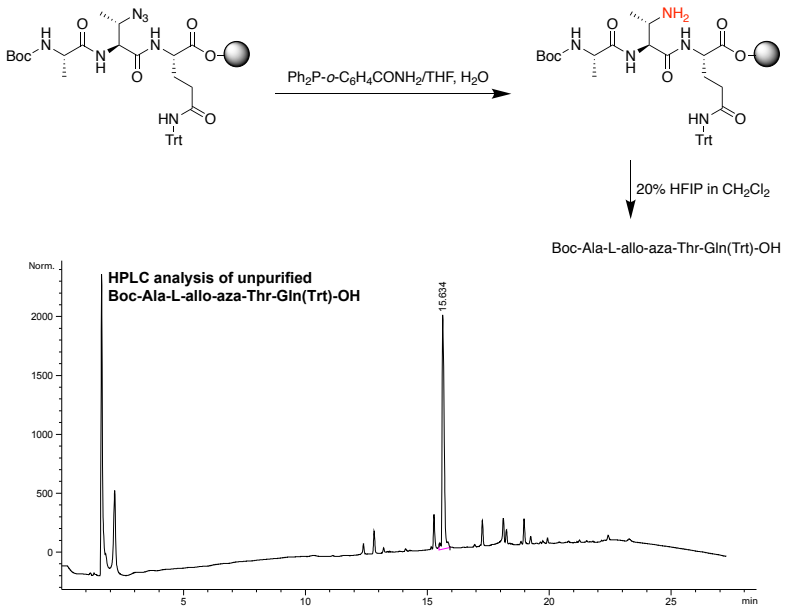

Figure S29. Analytical HPLC trace of Boc-Ala-L-*allo*-aza-Thr-Gln(Trt)-OH. Analytical RP-HPLC was performed on a C18 column with an elution gradient of 5-100% CH_3CN over 20 min.

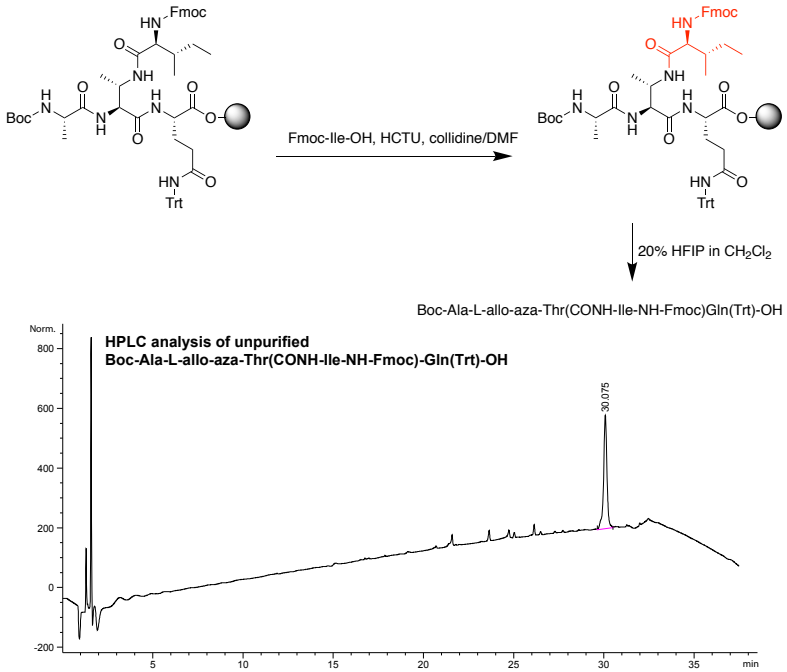

Figure S30. Analytical HPLC trace of Boc-Ala-L-*allo*-aza-Thr(CONH-Ile-NH-Fmoc-Gln(Trt)-OH. Analytical RP-HPLC was performed on a C18 column with an elution gradient of 5-100% CH_3CN over 30 min.

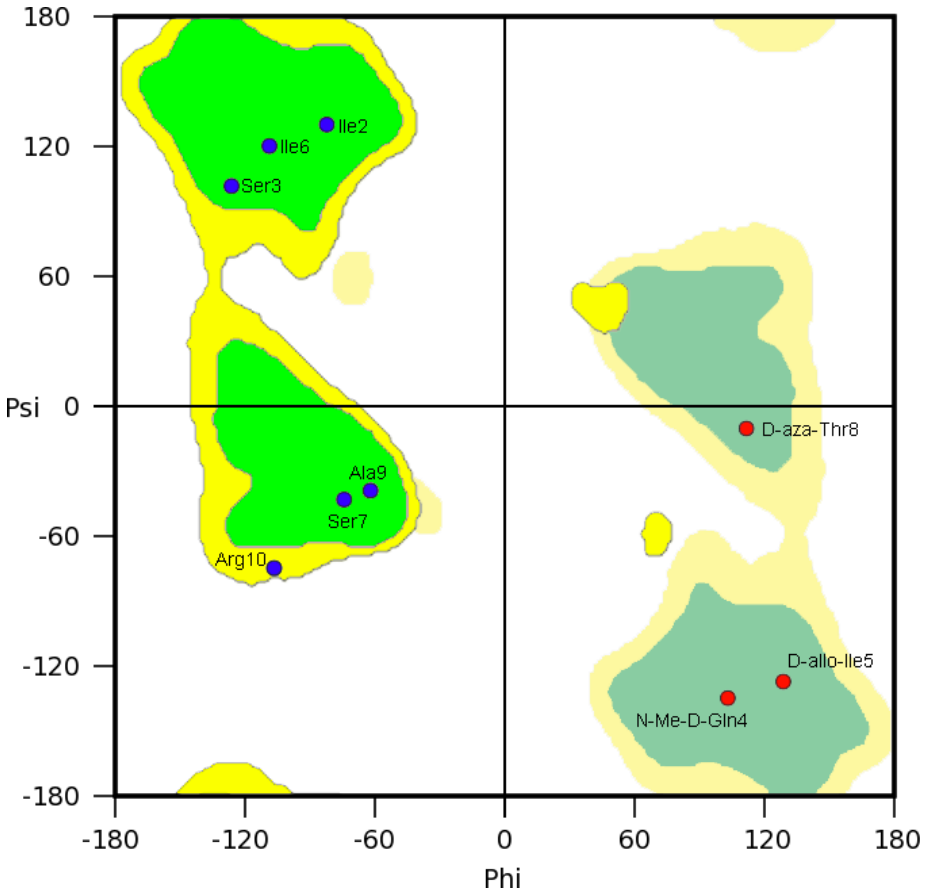

Figure S31. Ramachandran plot illustrating the ϕ and φ angles of residues 2–10 of *N*-Me-D-Gln$_4$,D-aza-Thr$_8$,Arg$_{10}$-teixobactin (**3a**). The green regions correspond to preferred dihedral angles for L-peptides and proteins; the yellow regions correspond to allowed regions for L-peptides and proteins; the pastel green and pastel yellow regions correspond to preferred and allowed dihedral angles for D-peptides and proteins.

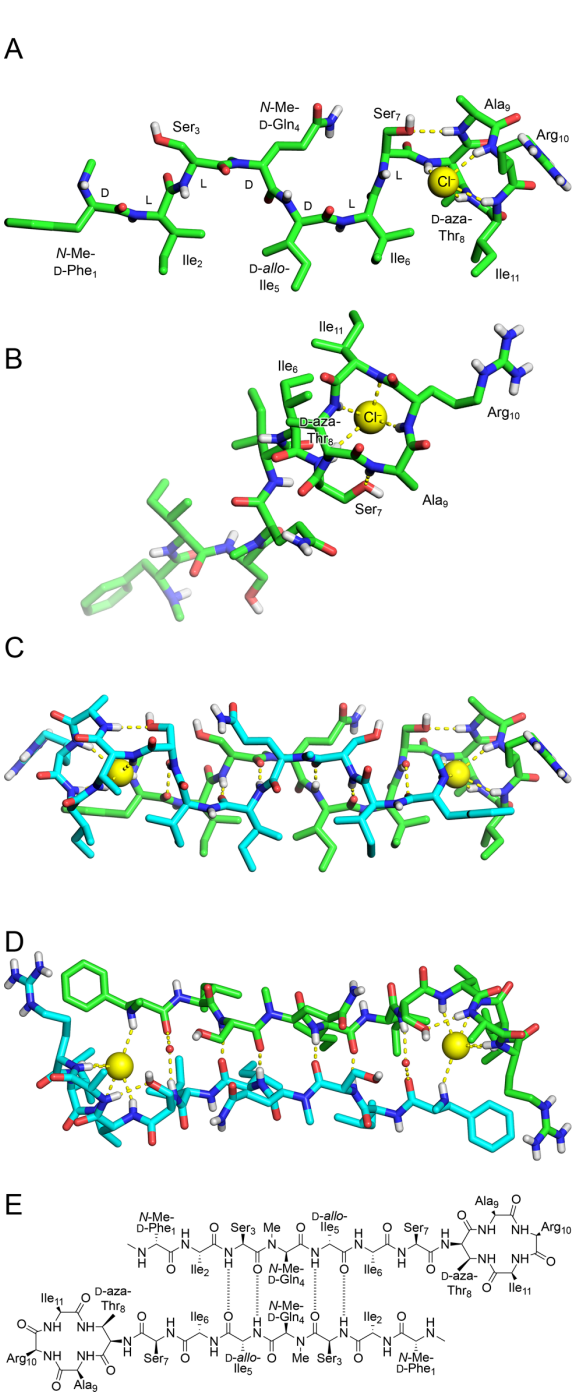

Figure 4. X-ray crystallographic structure of *N*-Me-D-Gln$_4$,D-aza-Thr$_8$,Arg$_{10}$-teixobactin (**3a**) binding chloride anions (PDB 6PSL). (A and B) Monomer side and top views. (C and D) Dimer side and top views with two bridging water molecules shown as non-bonded spheres. (E) Alignment of the dimer assembly.

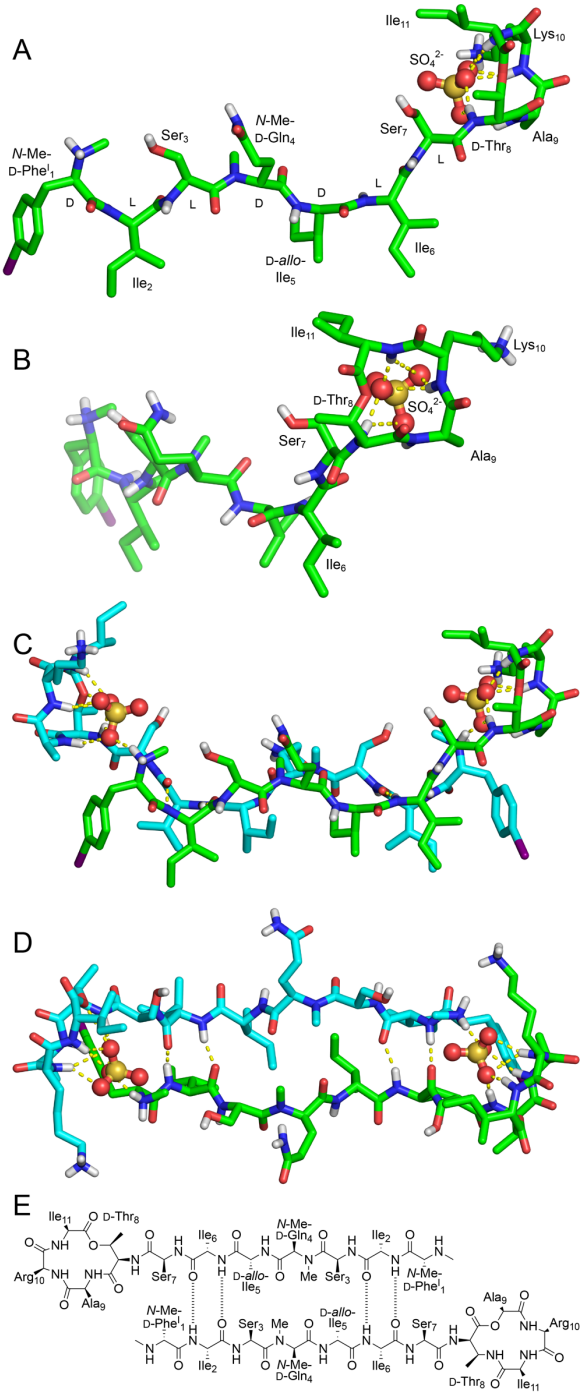

Figure S32. X-ray crystallographic structure of *N*-Me-D-Phe$^{I}_1$,*N*-Me-D-Gln$_4$,Lys$_{10}$-teixobactin binding sulfate anions (PDB 6E00). (A and B) Monomer side and top views. (C and D) Dimer side and top views. (E) Alignment of the dimer assembly.

Molecular Modeling Studies. Molecular modeling studies suggest that the methyl group of D-Thr$_8$ is important in controlling the conformation of the macrocyclic ring of teixobactin (Figure S33). Conformational searching of a truncated homologue of teixobactin containing alanine side chains, Ac-cyclo(D-Thr$_8$-Ala$_9$-Ala$_{10}$-Ala$_{11}$), revealed a single low-energy conformer within 5 kJ/mol, while conformational searching of Ac-cyclo(D-Dap$_8$-Ala$_9$-Ala$_{10}$-Ala$_{11}$) found multiple low-energy conformers. Conformational searching of Ac-cyclo(D-aza-Thr$_8$-Ala$_9$-Ala$_{10}$-Ala$_{11}$ afforded only two low-energy conformers, with the NH groups aligning in both conformers to create a potential binding site for anions. Molecular modeling studies of ring-expanded analogues containing one, two, or three β^3-homo amino acids at positions 9, 10, and 11 suggest that the ring expanded analogues are more flexible than teixobactin or Arg$_{10}$-teixobactin and that the NH groups of the rings are less well aligned to bind anions (Figure S34).

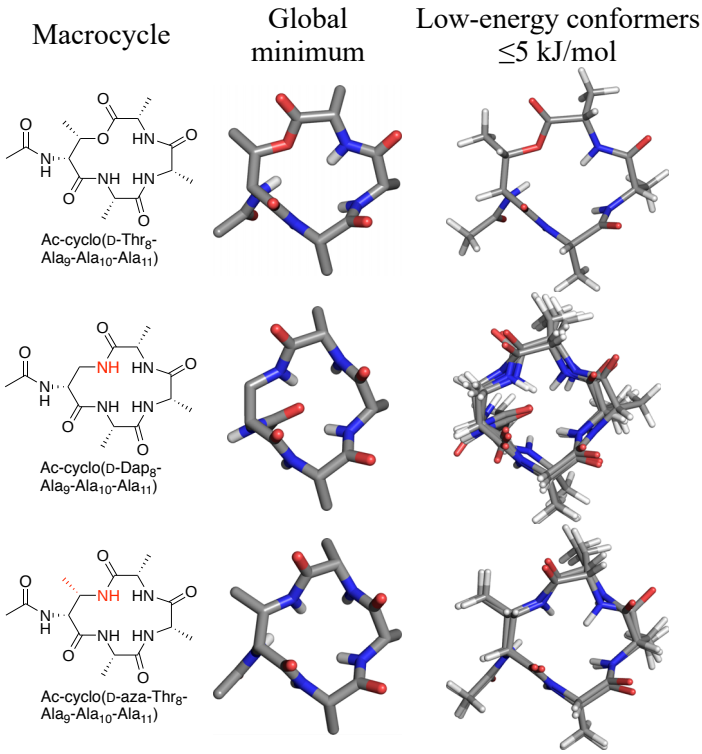

Figure S33. Molecular models of low-energy conformers of macrocycles from teixobactin and aza-teixobactin analogues. The models were generated by conformational searching in MacroModel using the MMFFs force field and GB/SA water solvation. Conformers represent the global minimum and all low-energy conformers within 5.0 kJ/mol of the global minimum.

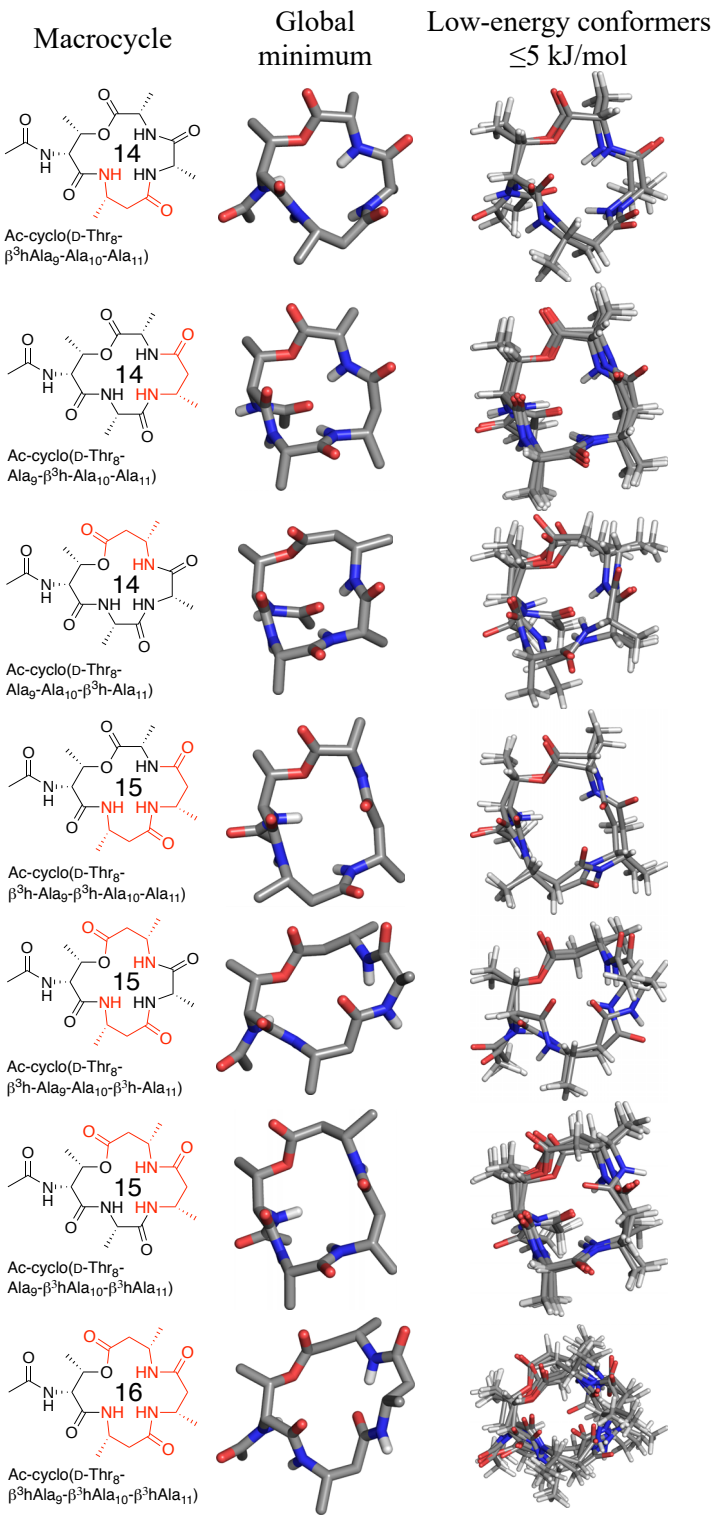

Figure S34. Molecular models of low-energy conformers of macrocycles from ring-expanded macrolactone teixobactin analogues containing β^3-homo alanine residues. The models were generated by conformational searching in MacroModel using the MMFFs force field and GB/SA water solvation. Conformers represent the global minimum and all low-energy conformers within 5.0 kJ/mol of the global minimum.

Table S1. MIC values of ring-expanded teixobactin analogues (μg/mL) with 0.002% polysorbate 80.

	Staphylococcus epidermidis ATCC 14990	*Bacillus subtilis* ATCC 6051	*Escherichia coli* ATCC 10798
Arg_{10}-teixobactin (**1a**)	0.13	0.06	>8
β^3h-Ala,Arg_{10}-teixobactin (**4**)	4	8	>8
β^3h-Arg_{10}-teixobactin (**5**)	0.13	0.13	>8
Arg_{10},β^3h-Ile_{11}-teixobactin (**6**)	2	2	>8
β^3h-Ala_9,β^3h-Arg_{10}-teixobactin (**7**)	>8	>8	>8
β^3h-Ala_9,Arg_{10},β^3h-Ile_{11}-teixobactin (**8**)	>8	>8	>8
β^3h-Arg_{10},β^3h-Ile_{11}-teixobactin (**9**)	0.13	0.13	>8
β^3h-Ala_9,β^3h-Arg_{10},β^3h-Ile_{11}-teixobactin (**10**)	2	4	>8
teixobactin	<0.008	<0.008	>8
vancomycin	0.25	0.25	>8

Materials and Methods

General information

Methylene chloride (CH_2Cl_2) was passed through alumina under argon prior to use. Amine-free *N*,*N*-dimethylformamide (DMF) was purchased from Alfa Aesar. Fmoc-D-*allo*-Ile-OH was purchased from Santa Cruz Biotechnology. Fmoc-*N*-Me-D-Gln(Trt)-OH was purchased from ChemPep. Other protected amino acids were purchased from CHEM-IMPEX. 2-(Diphenylphosphino)benzoic acid was purchased from Arctom chemicals. Preparative reverse-phase HPLC was performed on a Rainin Dynamax instrument equipped with an Agilent Zorbax SB-C18 column. Analytical reverse-phase HPLC was performed on an Agilent 1260 Infinity II instrument equipped with a Phenomonex Aeris PEPTIDE 2.6μ XB-C18 column. HPLC grade acetonitrile (MeCN) and deionized water (18 MΩ) containing 0.1% trifluoroacetic acid (TFA) were used as solvents for both preparative and analytical reverse-phase HPLC. Deionized water (18 MΩ) was obtained from a Barnstead NANOpure Diamond purification system or a ThermoScientific Barnstead GenPure Pro water purification system. Glass solid-phase peptide synthesis vessels with fritted disks and BioRad Polyprep columns were used for solid-phase peptide synthesis. Teixobactin analogues **2a–10** were prepared and studied as the trifluoroacetate salts.

Synthesis of D-aza-Thr$_8$,Arg$_{10}$-teixobactin (2a)[1]

Resin Loading. 2-Chlorotrityl chloride resin (300 mg, 1.2 mmol/g) was added to a 10-mL Bio-Rad Poly-Prep chromatography column. The resin was suspended in dry CH_2Cl_2 (5 mL) and allowed to swell for 15 min. The CH_2Cl_2 was drained with a flow of nitrogen. The resin was loaded with a solution of Fmoc-Ala-OH (90 mg, 0.29 mmol) and 2,4,6-collidine (300 μL) in dry CH_2Cl_2 (7 mL) and rocked for 4 h.

Resin Capping. The solution was drained with a flow of nitrogen, and the resin was washed with dry CH_2Cl_2 (3x). A mixture of CH_2Cl_2 (5 mL), MeOH (0.8 mL), and DIPEA (0.4 mL) was made and poured into the Poly-Prep column containing the resin, and the column was rocked for 1 h to cap any unreacted sites in the resin. The solution was drained with a flow of nitrogen, and the resin was washed with dry CH_2Cl_2 (3x). The resin was washed with MeOH and blown with nitrogen until dry resin was observed.

Loading check. Approximately 1 mg of the dry resin was weighed out into a scintillation vial and 20% piperidine in DMF (3 mL) was added. The vial was rocked for 30 min. The mixture was filtered using a Pasteur pipet plugged with glass wool. The UV/Vis spectrometer was blanked at 290 nm with a cuvette filled with 20% piperidine in DMF. The absorbance of the filtered mixture was measured [1.4 mg of resin weighed; A_{290} = 1.1234; 0.15 mmol loading].

Fmoc deprotection. The loaded resin was transferred to a solid-phase peptide hand coupling vessel. The resin was washed with dry CH_2Cl (3x) and then dry DMF (3x). To the reaction vessel, 20% piperidine in dry DMF (5 mL) was added. Using a nitrogen flow to bubble the hand coupling vessel, the reaction was mixed for 20 min. The resin was washed with dry DMF (3x).

Coupling Fmoc-D-allo-Thr-OH with HCTU. Based on loading, Fmoc-D-*allo*-Thr-OH (105 mg, 0.30 mmol, 2 equiv) and HCTU (121 mg, 0.30 mmol, 2 equiv) were weighed out and dissolved in 20% collidine in dry DMF. This solution was added to the reaction vessel containing the deprotected peptide on resin. Using a nitrogen flow to bubble the hand coupling vessel, the reaction was mixed for 4 h. The resin was washed with dry DMF (3x).

Fmoc deprotection. To the reaction vessel, 20% piperidine in dry DMF (5 mL) was added. Using a nitrogen flow to bubble the hand coupling vessel, the reaction was mixed for 20 min. The resin was washed with dry DMF (3x).

Alloc protection. The resin was transferred to a Poly-Prep column with dry DMF and the solution was drained with a flow of nitrogen. The resin was washed with dry CH_2Cl_2 (3x). To the resin in the Poly-Prep column, dry CH_2Cl_2 (5 mL), DIPEA (38 µL, 0.23 mmol, 1.5 equiv) and allyl chloroformate (23 µL, 0.23 mmol, 1.5 equiv) were added sequentially. The column was then capped and rocked for 1 h. The resin was washed with dry CH_2Cl (3x).

Mesylation. Dry CH_2Cl_2 (6 mL) was added to the resin in the Poly-Prep column. The column was then capped and rocked in a cold room (4 °C) for 15 min. DIPEA (254 µL, 1.5 mmol, 10 equiv) was added, and the mixture was rocked in a cold room (4 °C) for an additional 15 min. Methanesulfonyl chloride (113 µL, 1.5 mmol, 10 equiv) was added, and mixture was rocked in a cold room (4 °C) for an additional 15 min. The resin was then washed with dry CH_2Cl_2 (3x) and then with dry DMF (3x). The resin was transferred to the hand coupling vessel.

S_N2 with NaN_3. NaN_3 (474 mg, 7.5 mmol, 50 equiv) was added to the resin in the hand coupling vessel. Dry DMF (1 mL) and 15-crown-5 (1 mL) were added to the hand coupling vessel. [Not all of the NaN_3 dissolves in the solvent mixture.] Plastic tubing with a continuous water flow at 55 °C was wrapped around the hand coupling vessel to provide heating. Using a gentle nitrogen flow, the mixture was bubbled for 12 h at 55 °C. The resin was washed with 10 mL of 20% H_2O in THF (5x) to remove excess NaN_3. The resin was transferred to a Poly-Prep column with dry DMF and then washed with dry CH_2Cl_2 (3x).

Alloc deprotection. A mixture of CH_2Cl_2 (5 mL), $(Ph_3P)_4Pd$ (16.9 mg, 0.015 mmol, 0.1 equiv) and $PhSiH_3$ (360 µL, 3 mmol, 20 equiv) was added to the resin in the Poly-Prep column, and the column was rocked for 30 min. The resin was washed with dry CH_2Cl_2 (3x) and then with dry DMF (3x) and transferred to a hand coupling vessel.

Peptide coupling. The linear peptide was synthesized through the following cycles: *i*. coupling of amino acid (0.60 mmol, 4 equiv) with HCTU (241 mg, 0.60 mmol, 4 equiv) in 20%

(v/v) 2,4,6-collidine in dry DMF (3 mL) for 30 min, *ii*. resin washing with dry DMF (3x), *iii*. Fmoc deprotection with 20% (v/v) piperidine in dry DMF (3 mL) for 20 min, and *iv*. resin washing with dry DMF (3x). For D-to-L and L-to-D amino acid couplings, the reaction time in step *i* was increased to 1 h. After completing the linear synthesis, the resin was transferred to a 10-mL Bio-Rad Poly-Prep chromatography column. The resin was then washed with dry DMF (3x) and then dry THF (3x).

Azide reduction. Triphenylphosphine-2-carboxamide[2] (223 mg, 0.45 mmol, 5 equiv) in THF (5 mL) was added to the resin in a Poly-Prep column, and the column was rocked for 12 h. The solution was drained with a flow of nitrogen and 20% H_2O in THF (5 mL) was added and rocked for 4 h. The resin was washed with dry DMF (3x) and transferred to a hand coupling vessel using DMF.

Peptide coupling. The coupling and Fmoc deprotection of Ile_{11} and Arg_{10} was performed as described above. After Fmoc deprotection of Arg_{10}, the resin containing branched linear peptide was transferred to 10-mL Bio-Rad Poly-Prep chromatography column using DMF. The resin was washed with dry DMF (3x) and then with dry CH_2Cl_2 (3x).

Cleavage of the branched linear peptide from the resin. The protected peptide was cleaved from the resin by adding 20% hexafluoroisopropanol in dry CH_2Cl_2 (7 mL) to the column and rocking for 30 min. The filtrate was collected in a round-bottom flask. The resin was washed with a second aliquot of 20% hexafluoroisopropanol (7 mL). The filtrates were combined and concentrated under reduced pressure to afford a clear oil. The oil was placed under vacuum (≤ 100 mTorr) to remove any residual solvents.

Macrolactamization. To the round-bottom flask containing cleaved peptide, a mixture of HBTU (332 mg, 0.9 mmol, 6 equiv) and HOBT (118 mg, 0.9 mmol, 6 equiv) in dry DMF (50 mL) was added and stirred for 15 min under nitrogen. Diisopropylethylamine (153 μL, 0.9 mmol, 6

equiv) was added to the stirring solution and then stirred for 12 h under nitrogen. The solution was evaporated by rotary evaporator and the residue was dried under vacuum (≤ 100 mTorr) to give a pale-yellow pellet.

Global deprotection. A solution of TFA (9 mL), H_2O (0.5 mL), and TIPS (0.5 mL) was added to the round-bottom flask containing cyclized peptide and stirred for 1 h under nitrogen. The solution was evaporated by rotary evaporator and the residue was dried under vacuum (≤ 100 mTorr).

Purification. The globally deprotected peptide was dissolved in approximately 35% CH_3CN in H_2O (10 mL), and the solution was centrifuged at 14,000 rpm for 5 min. The solution was filtered through a 0.20-μm nylon filter. The peptide was purified by reverse-phase HPLC with H_2O/CH_3CN (gradient elution of 20-95% CH_3CN with 0.1% TFA). Pure fractions were identified by analytical HPLC and electrospray ionization (ESI) mass spectrometry and were combined and lyophilized. D-aza-Thr_8,Arg_{10}-teixobactin (**2a**) was isolated as trifluoroacetic acid (TFA) salt of a 13.5 mg white powder with ≥95% purity.

Synthesis of diastereomeric azateixobactin analogues (2b–2d)

Other diastereomeric azateixobactin analogues (**2b–2d**) were prepared using the procedures described above. Replacing D-*allo*-threonine with D-threonine in the synthesis afforded D-*allo*-aza-threonine and gave diastereomer **2b**. Replacing D-*allo*-threonine with L-*allo*-threonine in the synthesis afforded L-aza-threonine and gave diastereomer **2c**. Replacing D-*allo*-threonine with L-threonine in the synthesis afforded L-*allo*-aza-threonine and gave diastereomer **2d**. For synthesis of L-*allo*-aza-Thr_8,Arg_{10}-teixobactin (**2d**), the azide reduction with triphenylphosphine-2-carboxamide was performed for 24 h instead of 12 h. The stereoisomers containing L-aza-threonine and L-*allo*-aza-threonine (**2c** and **2d**) exhibited an exceptionally strong propensity to

form gels, making purification difficult and affording only low yields of these diastereomeric teixobactin analogues after purification by RP-HPLC.

Synthesis of *N*-Me-D-Gln$_4$,D-aza-Thr$_8$,Arg$_{10}$-teixobactin (3a)

N-Methylated azateixobactin analogue (**3a**) was prepared using the procedures described above. Coupling of Fmoc-Ser$_3$(tBu)-OH after *N*-Me-D-Gln$_4$ was performed using 4 equiv Fmoc-Ser$_3$(tBu)-OH with coupling reagent HATU (4 equiv), HOAt (4 equiv) in 20% (v/v) collidine in dry DMF (5 mL) for 12 h.

Synthesis of ring-expanded teixobactin analogues (4–10)

Ring-expanded teixobactin analogues containing β^3-homo amino acids (**4–10**) were synthesized using the procedures we have previously reported.[1] Dry DMF was used instead of a mixture of CH_3CN/THF/CH_2Cl_2 for the cyclization step.

Minimum inhibitory concentration (MIC) assay of teixobactin analogue

MIC assays of teixobactin and teixobactin analogues (**2a–10**) were performed using the procedure we have previously reported.[1,3]

Preparing the peptide analogue stock. Solutions of D-aza-Thr$_8$,Arg$_{10}$-teixobactin (**2a**), other teixobactin analogues (**2b–10**), teixobactin and vancomycin were prepared gravimetrically by dissolving an appropriate amount of peptide in an appropriate volume of sterile DMSO to make 20 mg/mL stock solutions. The stock solutions were stored at -20 °C for subsequent experiments.

Prior to transferring the peptide solution in broth to 96-well plates, the peptide solution was vigorously vortexed with a vortex mixer for ca. 30 seconds to ensure thorough dispersion and/or dissolution of teixobactin and teixobactin analogues, which have a propensity to form gels.

Serial dilution of peptides in a 96-well plate. In the serial dilution, the first well containing 200-uL peptide solution was mixed with pipette up and down at least ten times before moving to

the next well. In the following serial dilutions, each well was also mixed with pipette up and down at least ten times.

Performing the minimum inhibitory concentration (MIC) assays with Mueller-Hinton broth containing 0.002% polysorbate 80. Mueller-Hinton broth containing 0.002% (v/v) polysorbate 80 was autoclaved and used in the MIC assay. The broth was used to dilute the 20 mg/mL DMSO solution of teixobactin and teixobactin analogues to 16 μg/mL and then to serially dilute the peptide solutions in the 96-well plate to the following concentrations: 16, 8, 4, 2, 1, 0.5, 0.25, 0.13, 0.063, 0.031, and 0.016 μg/mL. Each well contained 100 μL of solution. The broth was used to dilute bacterial suspension OD_{600} of 0.075 and to further dilute the bacterial suspension to 1 x 10^6 CFU/mL. 100-μL aliquots of the diluted bacteria were added to each well to give final concentration of 5 x 10^5 CFU/mL and final peptide concentrations of 8, 4, 2, 1, 0.5, 0.25, 0.13, 0.062, 0.031, 0.016, and 0.008 μg/mL.

Crystallization of *N*-Me-D-Gln$_4$,D-aza-Thr$_8$,Arg$_{10}$-teixobactin (3a)[4]

N-Me-D-Gln$_4$,D-aza-Thr$_8$,Arg$_{10}$-teixobactin (**3a**) was dissolved in 0.2 micron syringe filtered NANOpure H_2O (10 mg/mL). Crystallization conditions were screened by screening in a 96-well plate format using three crystallization kits from Hampton Research (PEG/Ion, Index, and Crystal Screen). Each well was loaded with 100 μL of a different mother liquor solution from the kits. The hanging drops were set up using a TTP Labtech Mosquito® liquid handling instrument. Hanging drops were made by combining an appropriate volume of *N*-Me-D-Gln$_4$,D-aza-Thr$_8$,Arg$_{10}$-teixobactin (**3a**) with an appropriate volume of well solution to create three 150-nL hanging drops with 1:1, 1:2, and 2:1 peptide:well solution. Hexagonal prism -shaped crystals grew in all conditions that contained polyethylene glycol (PEG) and chloride salts.

Crystal growth was optimized using conditions containing HEPES Na, PEG 400 and $CaCl_2$. In the optimization, the HEPES Na (pH 5.5-8.0), $CaCl_2$, and PEG 400 concentrations were varied across the 4x6 matrix of a Hampton VDX 24-well plate to afford crystals suitable for X-ray diffraction. The hanging drops for these optimizations were prepared on glass slides by combining 1 or 2 μL of teixobactin solution with 1 or 2 μL of well solution in ratios of 1:1, 2:1, and 1:2. Crystals that formed were checked for diffraction using a Rigaku Micromax-007 HF diffractometer with a Cu anode at 1.54 Å. As a result of the optimization, 0.16 M $CaCl_2$, 0.1 M HEPES Na pH 7.00, and 24% PEG 400 afforded crystals suitable for X-ray diffraction.

X-ray crystallographic data collection, data processing, and structure determination

Data collection was performed with the BOS/B3 software at Advanced Light Source (ALS) using beamline 8.2.2 at a wavelength of 1.771190 Å (7000 eV). The rotation method was employed and three sets of 360 images each were collected at a 1.0º rotation interval (a total of three complete 360º rotations). The three sets were processed with XDS,[5] and the resulting datasets were merged with BLEND.[6] The structure was solved with SAD phasing implemented in the Hybrid Substructure Search (HySS)[7] module of the Phenix suite[8] using the anomalous signal from the chloride ion. The initial electron density maps were generated using the substructure coordinates as initial positions in Autosol[9]. The structure was then refined with Phenix.refine[10] under Phenix using Coot[11] for model building. All B-factors were refined isotropically and riding hydrogen atoms coordinates were generated geometrically. The bond length, angles, and torsions restraints for unnatural amino acids (*N*-Me-D-Gln, D-aza-Thr, and D-*allo*-Ile) were generated with eLBOW[12] under Phenix. We refined the *N*-methyl terminus (*N*-Me-D-Phe$_1$) as the free amine, rather than as the ammonium ion, because there is only a single chloride anion in the asymmetric unit, which balances the positive charge of the arginine sidechain. We found no electron density or voids in the lattice that could account for an additional anion.

Table S3. Crystallographic properties, crystallization conditions, data collection, and model refinement statistics for *N*-Me-D-Gln$_4$,D-aza-Thr$_8$,Arg$_{10}$-teixobactin (**3a**).

	N-Me-D-Gln$_4$,D-aza-Thr$_8$,Arg$_{10}$-teixobactin (**3a**)
PDB ID	6PSL
space group	$P3_221$
a, b, c (Å)	20.024, 20.024, 32.328
α, β, γ (˚)	90.0, 90.0, 120.0
peptides per asymmetric unit	1
crystallization conditions	0.16 M $CaCl_2$, 0.1 M HEPES Na pH 7.00, 24% PEG 400
Data collection	
wavelength (Å)	1.771190 Å (7000 eV)
resolution (Å)	15.28-2.10 (2.35-2.10)
total reflections	24455 (4809)
unique reflections	535 (144)
Multiplicity	45.7 (33.4)
completeness (%)	99.7 (100)
mean I/σ	78.2 (52.7)
R_{merge}	0.053 (0.066)
$R_{measure}$	0.053 (0.067)
$CC_{1/2}$	1.00 (0.999)
CC*	1.00 (1.00)
Refinement	
R_{work}	0.092 (0.12)
R_{free}	0.117 (0.19)
number of non-hydrogen atoms per ASU	94
RMS_{bonds}	0.014
RMS_{angles}	0.99
Ramachandran	
allowed (%)	100
outliers (%)	0
clashscore	0
average B-factor	8.89

HPLC and MS of teixobactin analogues (2a-10)

aza-D-Thr$_8$,Arg$_{10}$-teixobactin (**2a**)

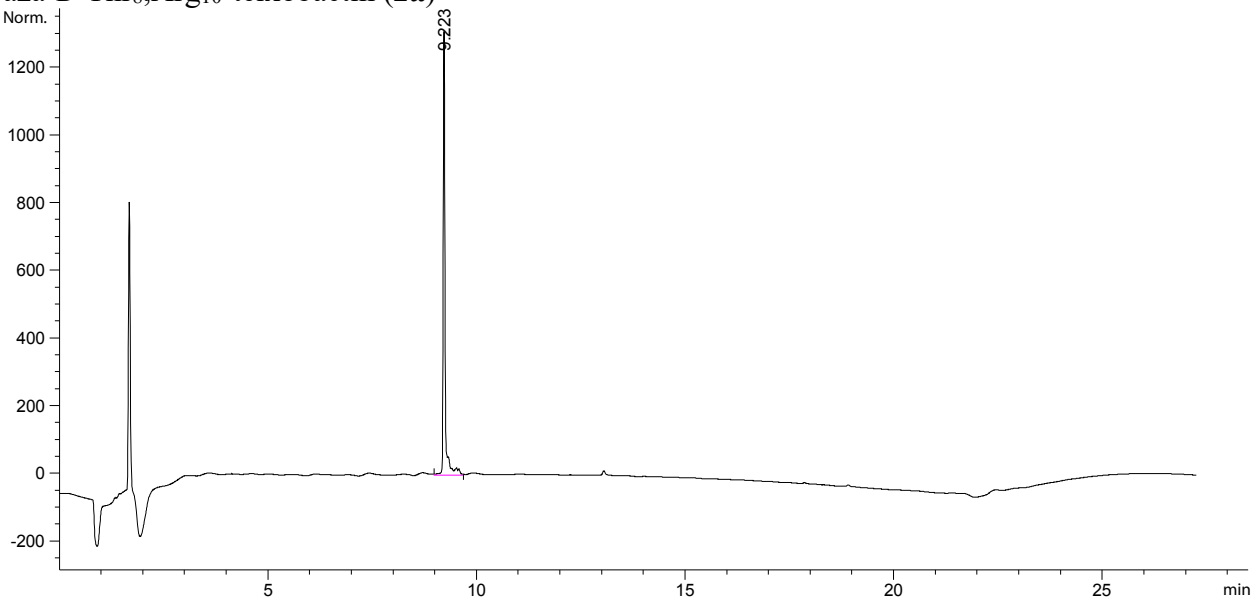

Analytical RP-HPLC was performed on a C18 column with an elution gradient of 5-100% CH_3CN over 20 min.

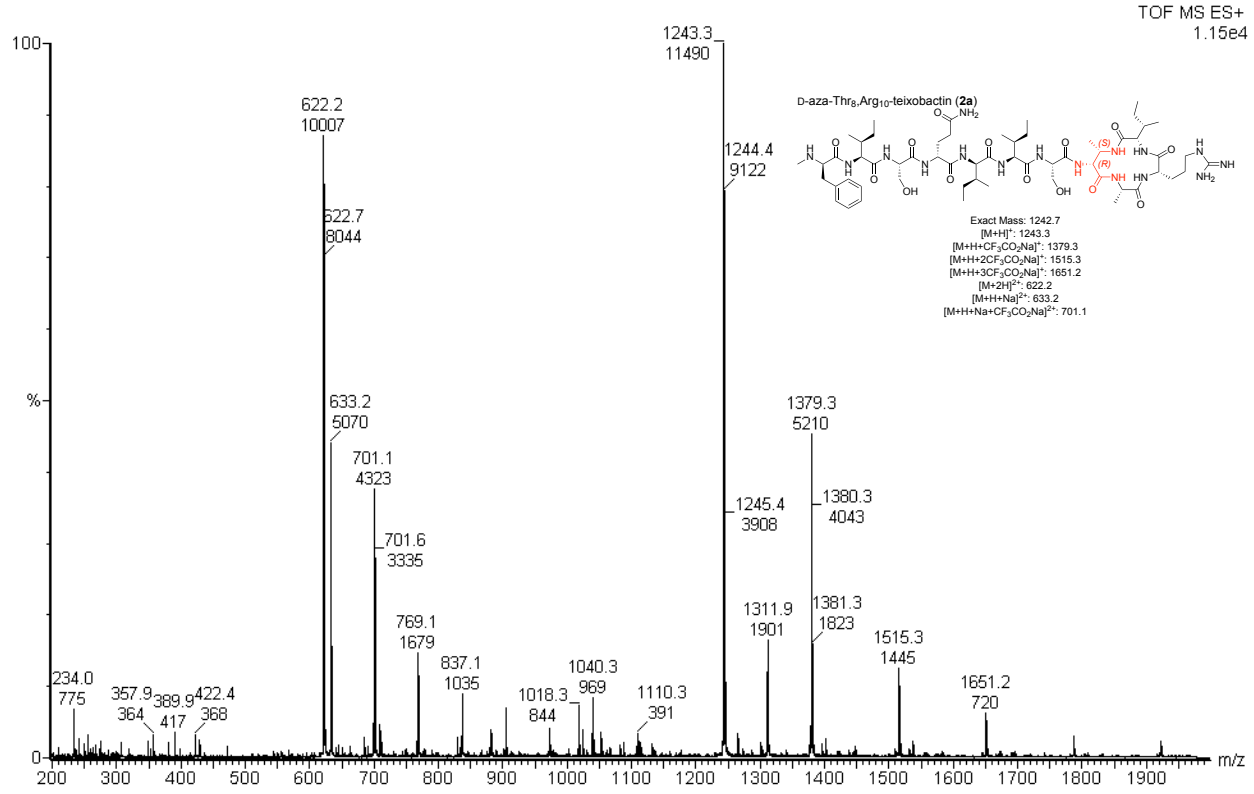

aza-D-*allo*-Thr$_8$,Arg$_{10}$-teixobactin (**2b**)

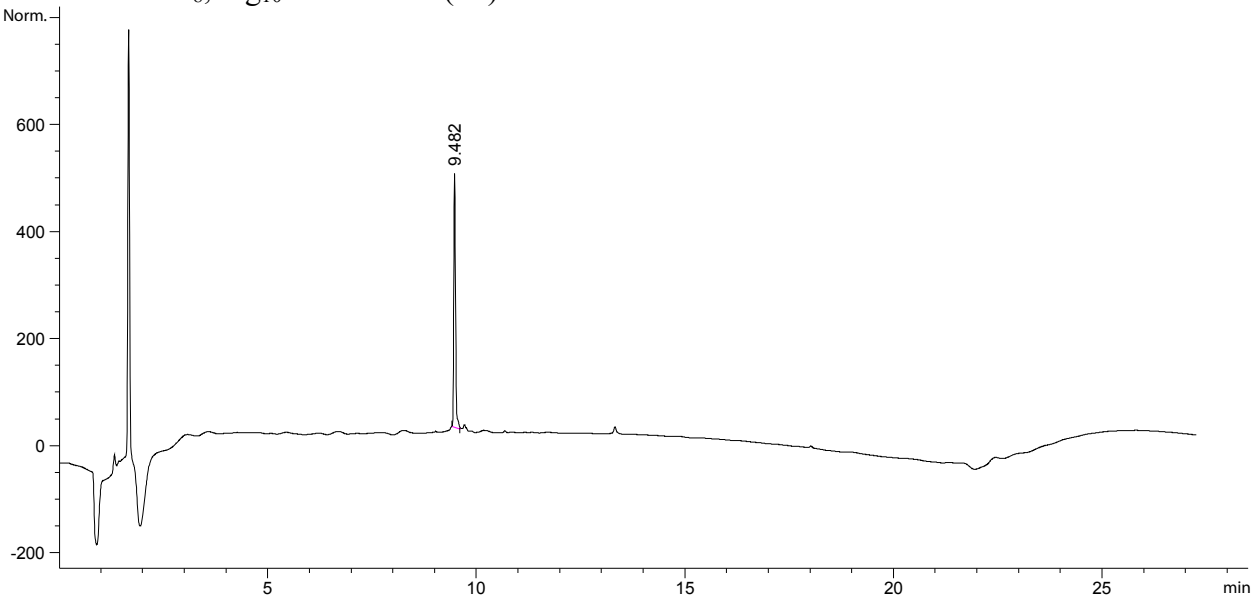

Analytical RP-HPLC was performed on a C18 column with an elution gradient of 5-100% CH_3CN over 20 min.

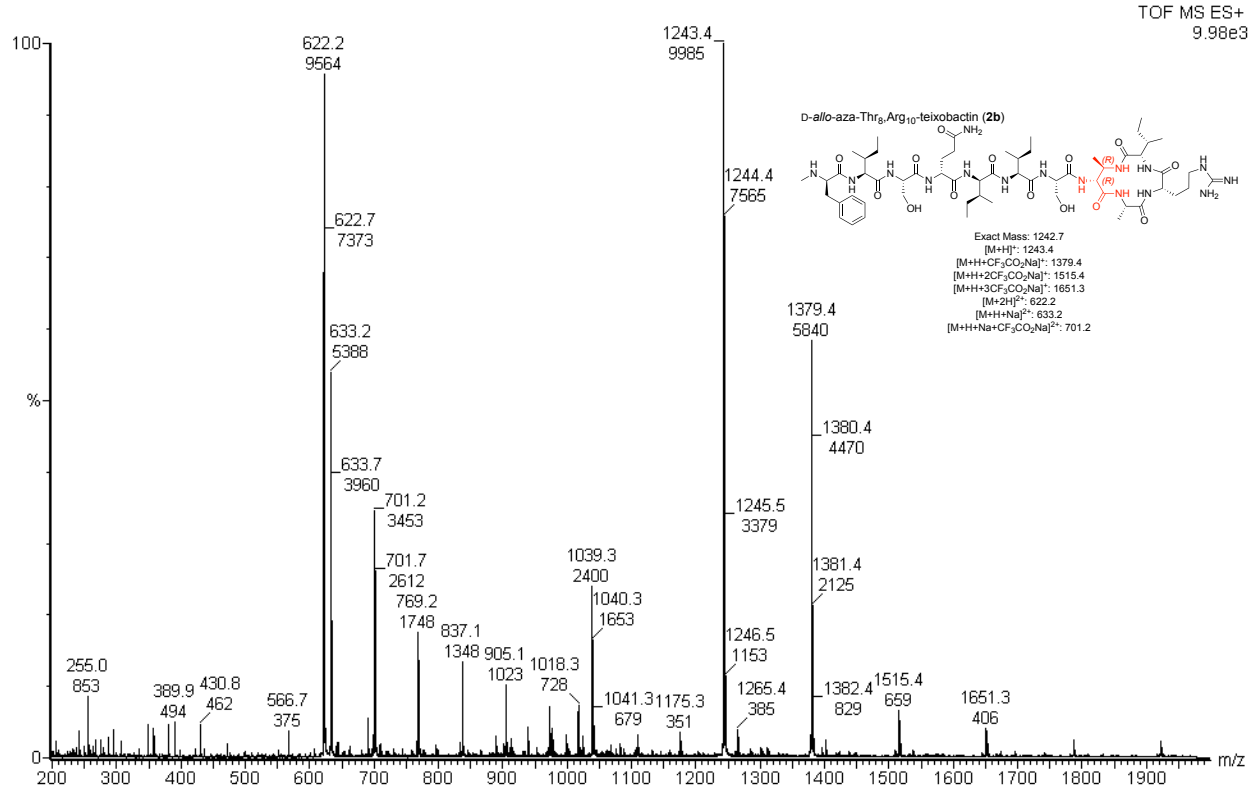

aza-L-Thr$_8$,Arg$_{10}$-teixobactin (**2c**)

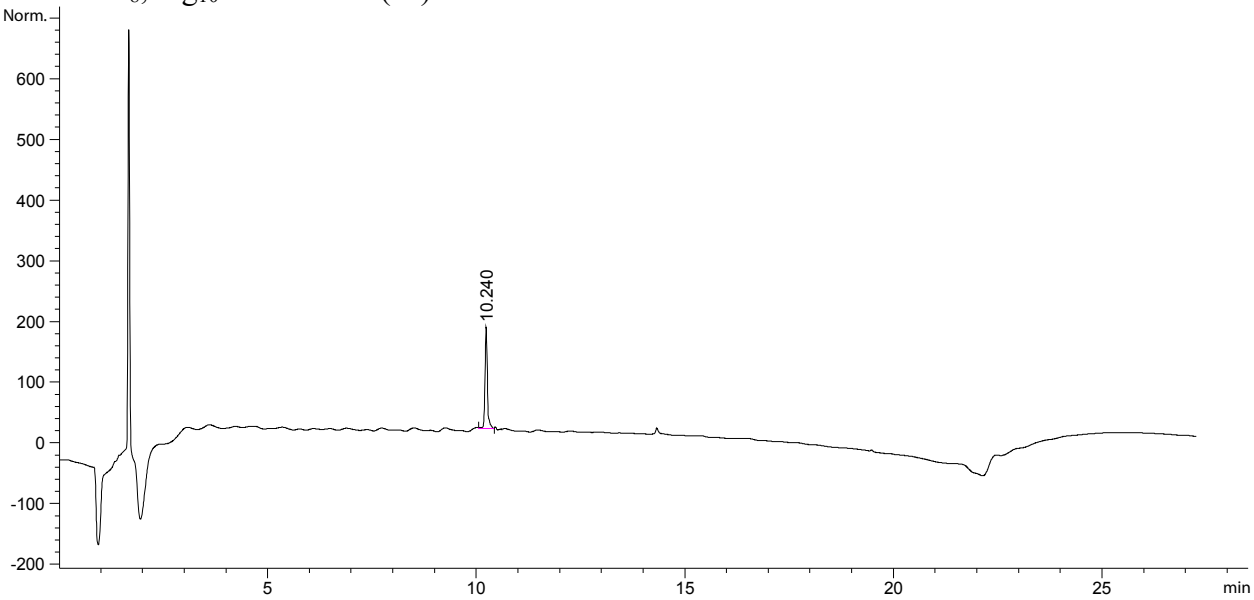

Analytical RP-HPLC was performed on a C18 column with an elution gradient of 5-100% CH_3CN over 20 min.

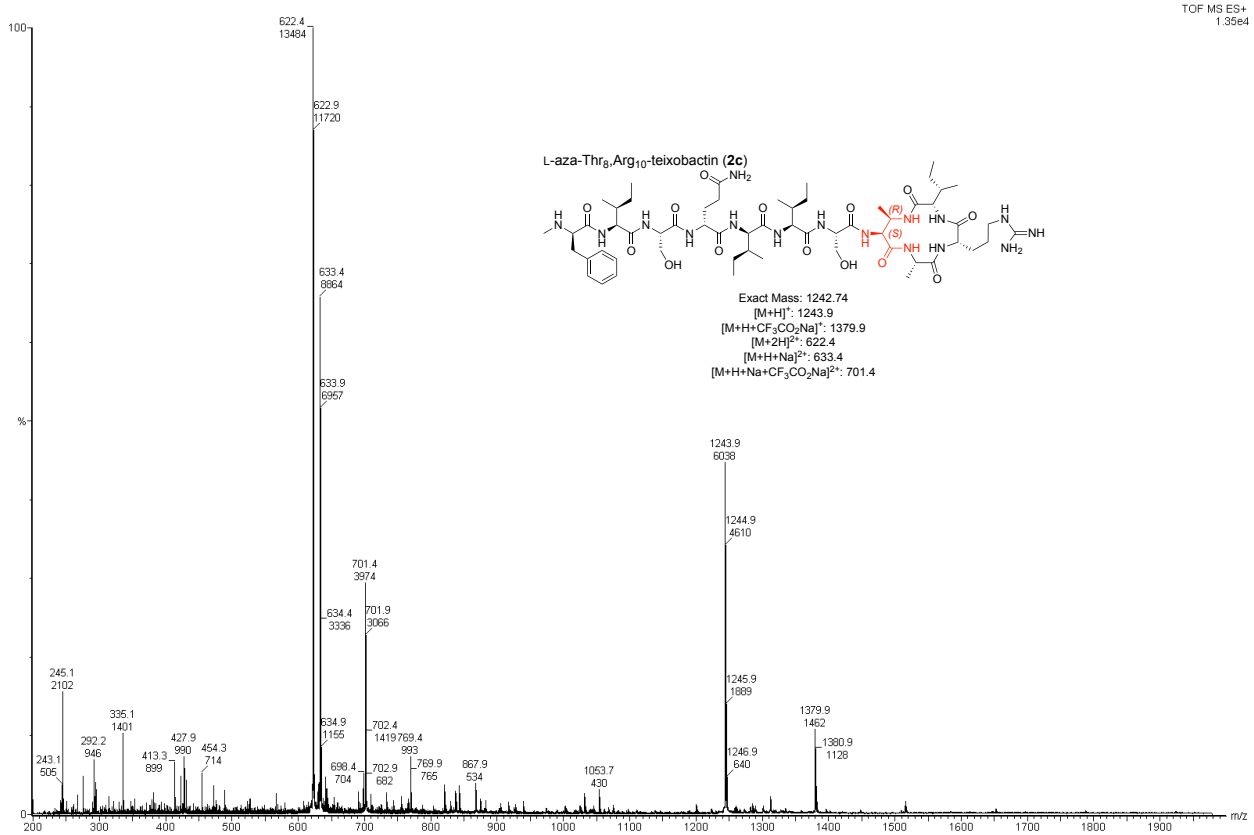

aza-L-*allo*-Thr$_8$,Arg$_{10}$-teixobactin (**2d**)

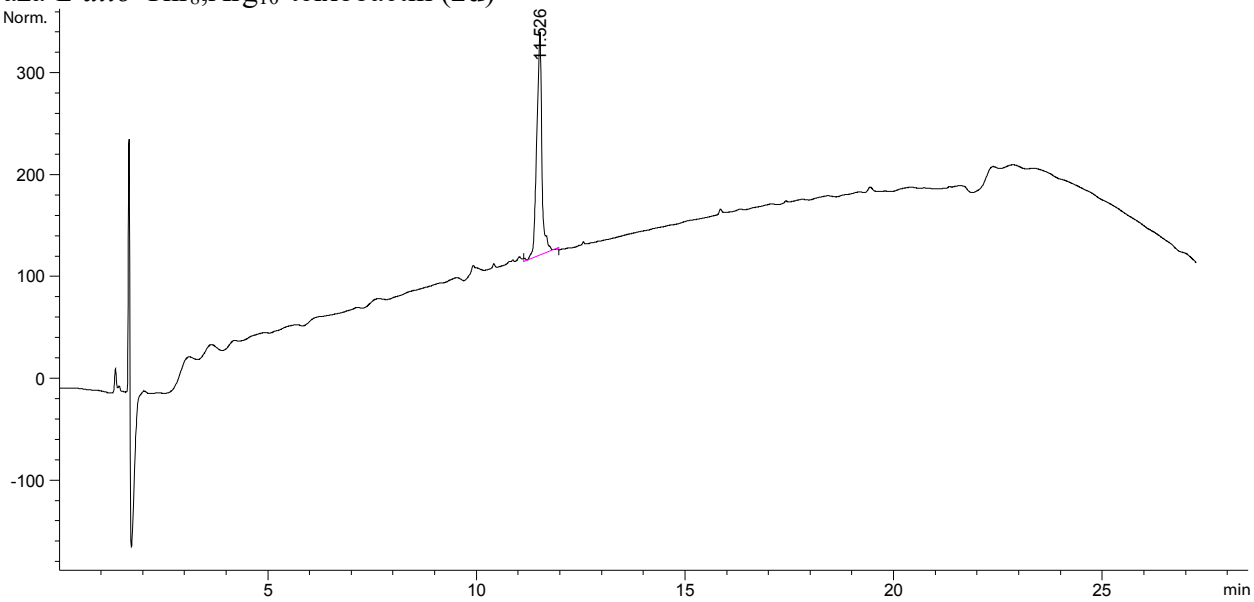

Analytical RP-HPLC was performed on a C18 column with an elution gradient of 5-100% CH_3CN over 20 min.

Applied Biosystems MDS Analytical Technologies TOF/TOF™ Series Explorer™ 72039

TOF/TOF™ Reflector Spec #1[BP = 1243.6, 158]

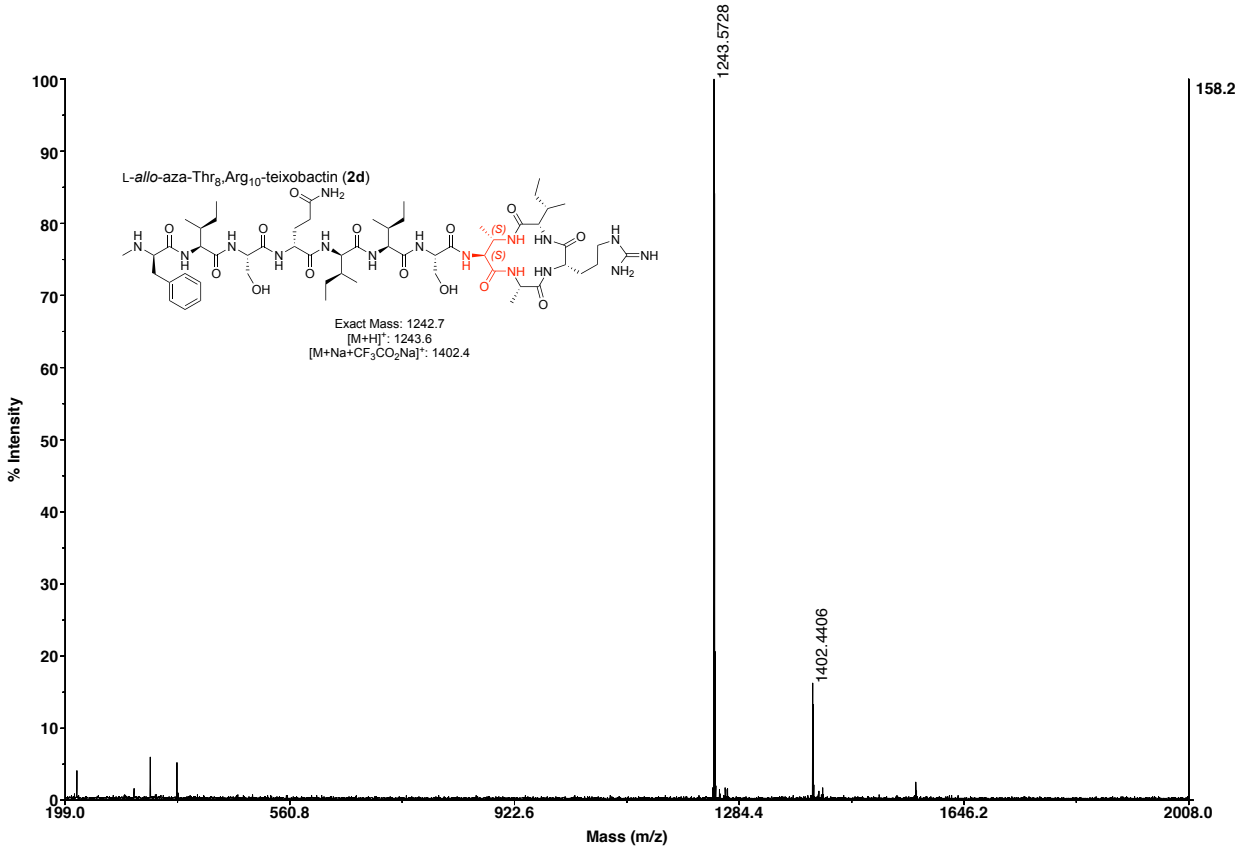

N-Me-D-Gln$_4$,aza-D-Thr$_8$,Arg$_{10}$-teixobactin (**3a**)

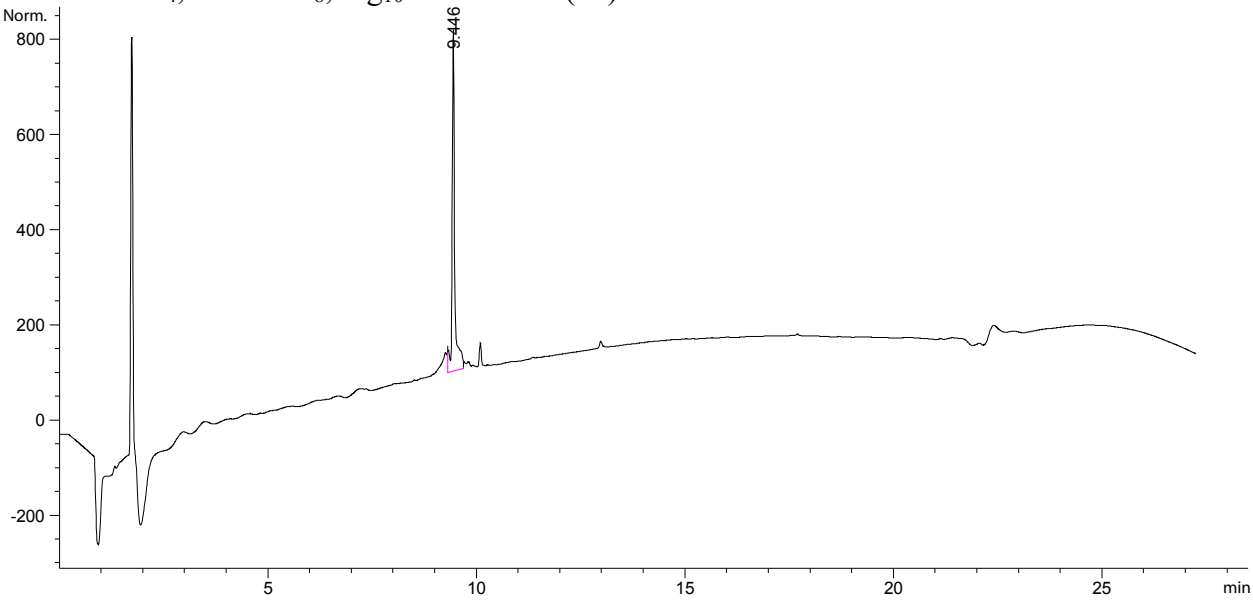

Analytical RP-HPLC was performed on a C18 column with an elution gradient of 5-100% CH_3CN over 20 min.

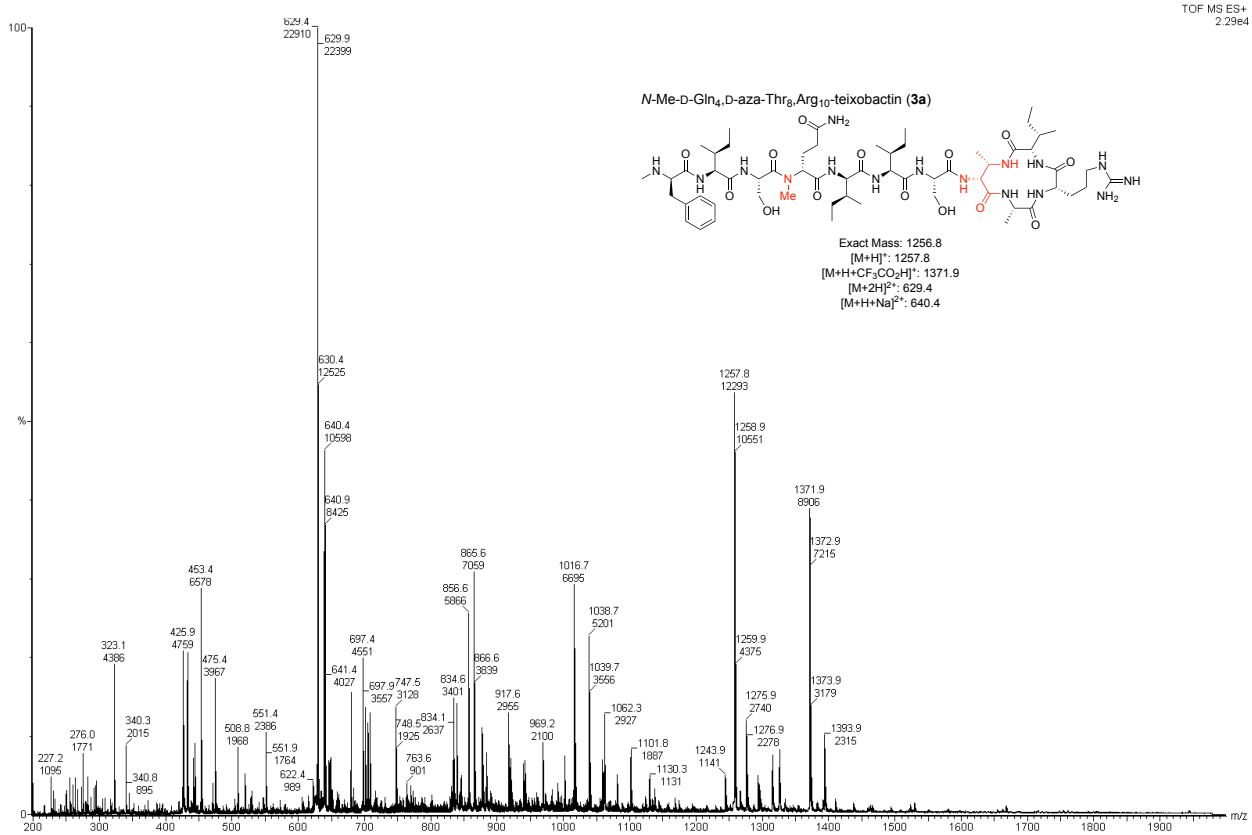

β^3h-Ala$_9$,Arg$_{10}$-teixobactin (**4**)

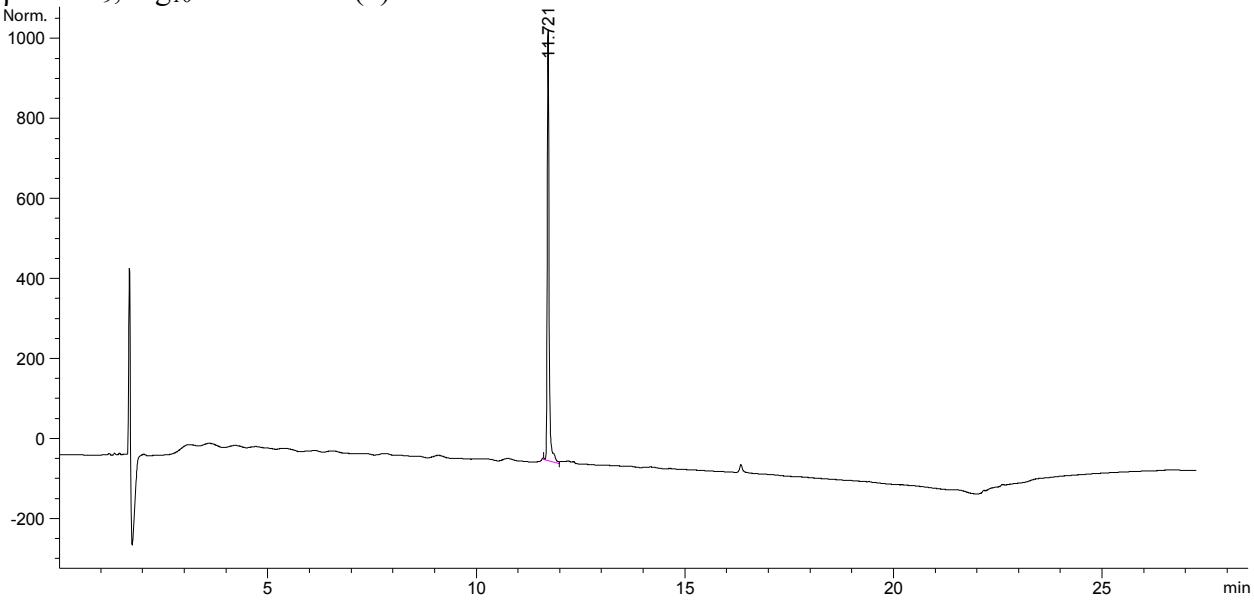

Analytical RP-HPLC was performed on a C18 column with an elution gradient of 5-100% CH_3CN over 20 min.

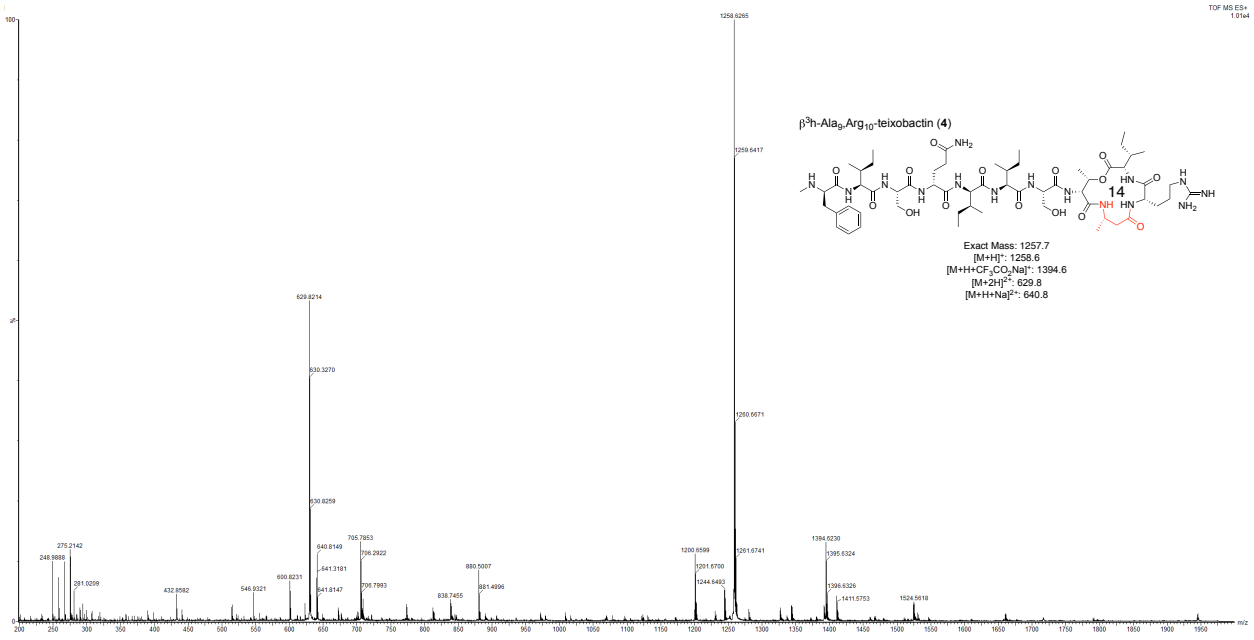

β^{3}h-Arg$_{10}$-teixobactin (**5**)

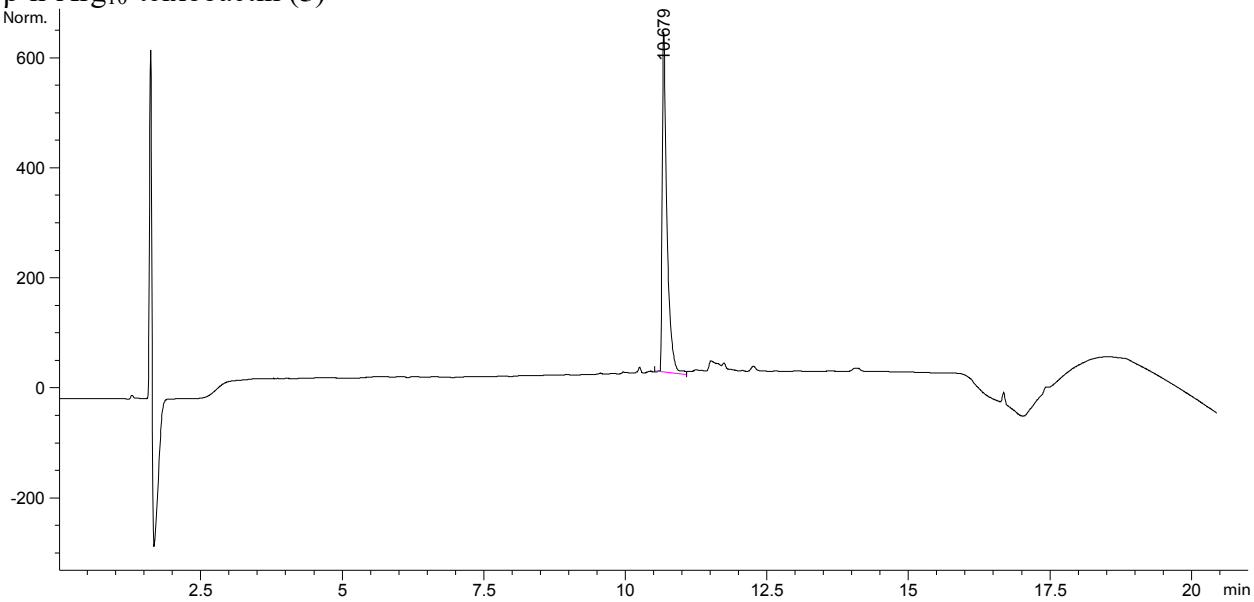

Analytical RP-HPLC was performed on a C18 column with an elution gradient of 5-67% CH_3CN over 15 min.

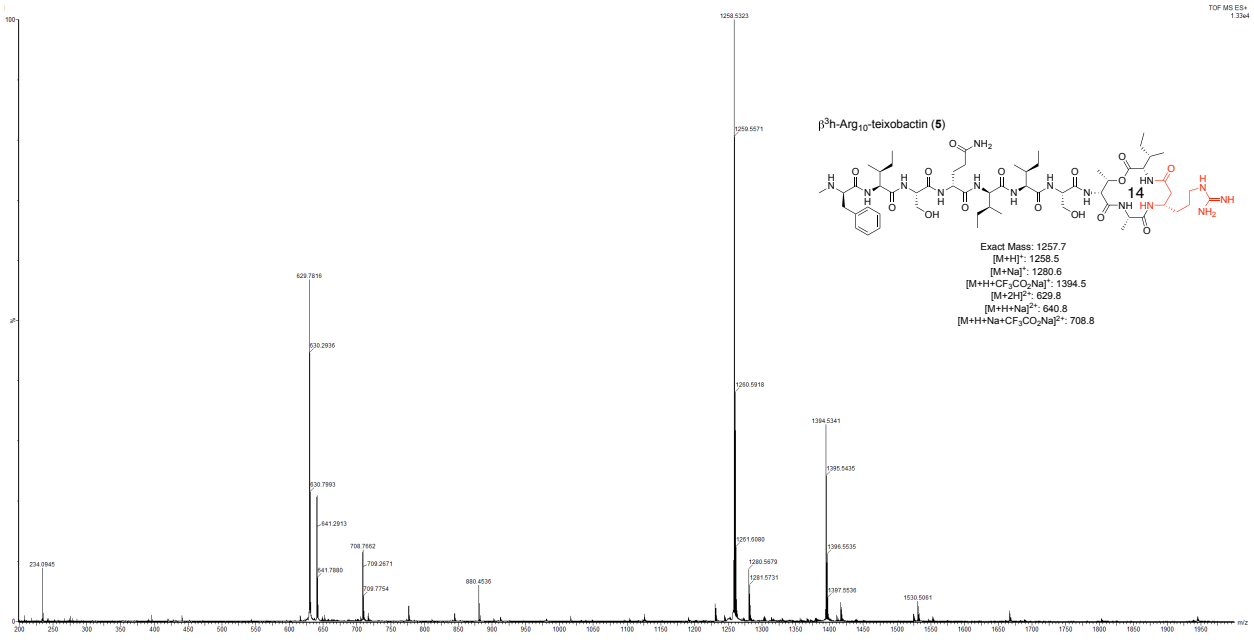

Arg_{10},β^3h-Ile_{11}-teixobactin (**6**)

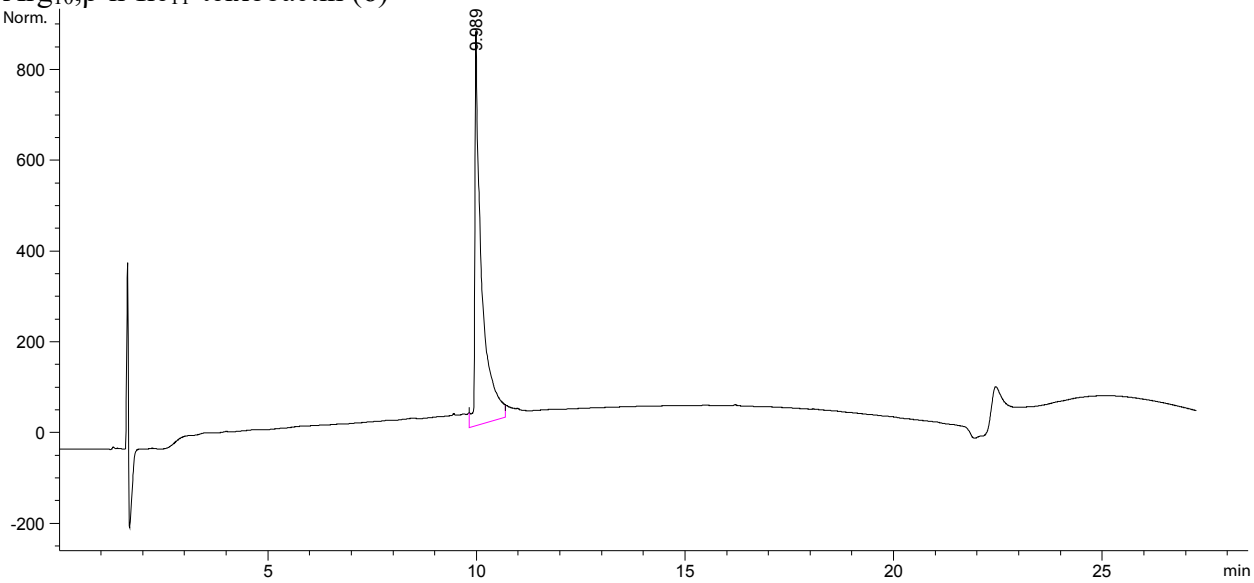

Analytical RP-HPLC was performed on a C18 column with an elution gradient of 5-100% CH_3CN over 20 min.

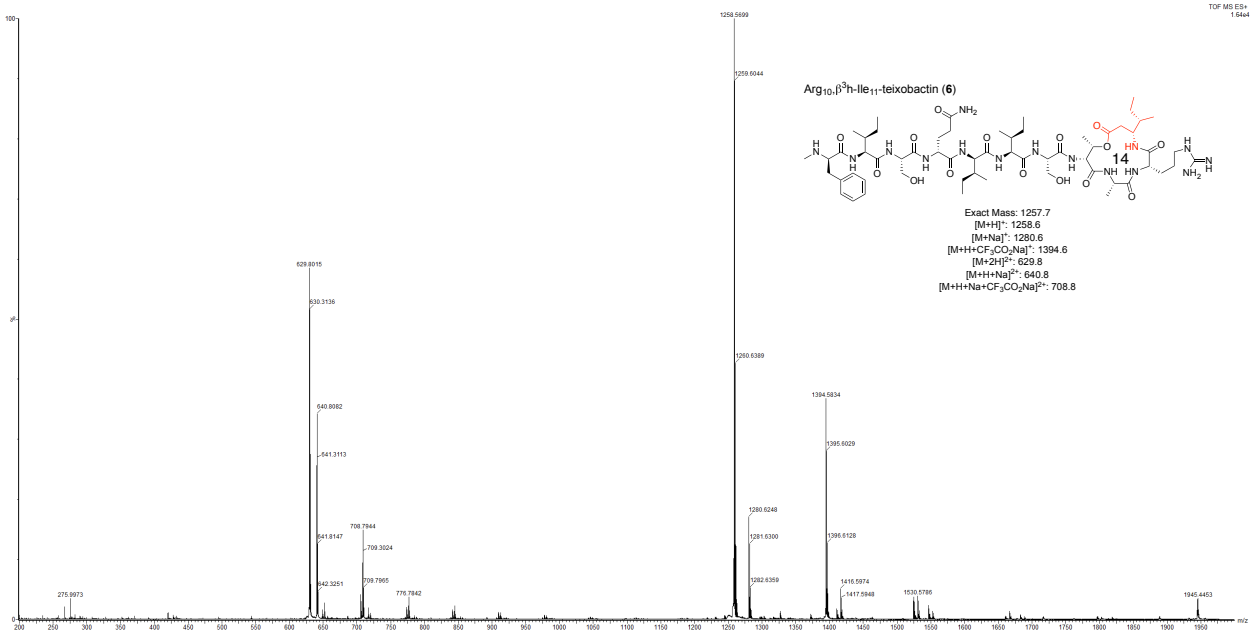

β^3h-Ala$_9$,β^3h-Arg$_{10}$-teixobactin (**7**)

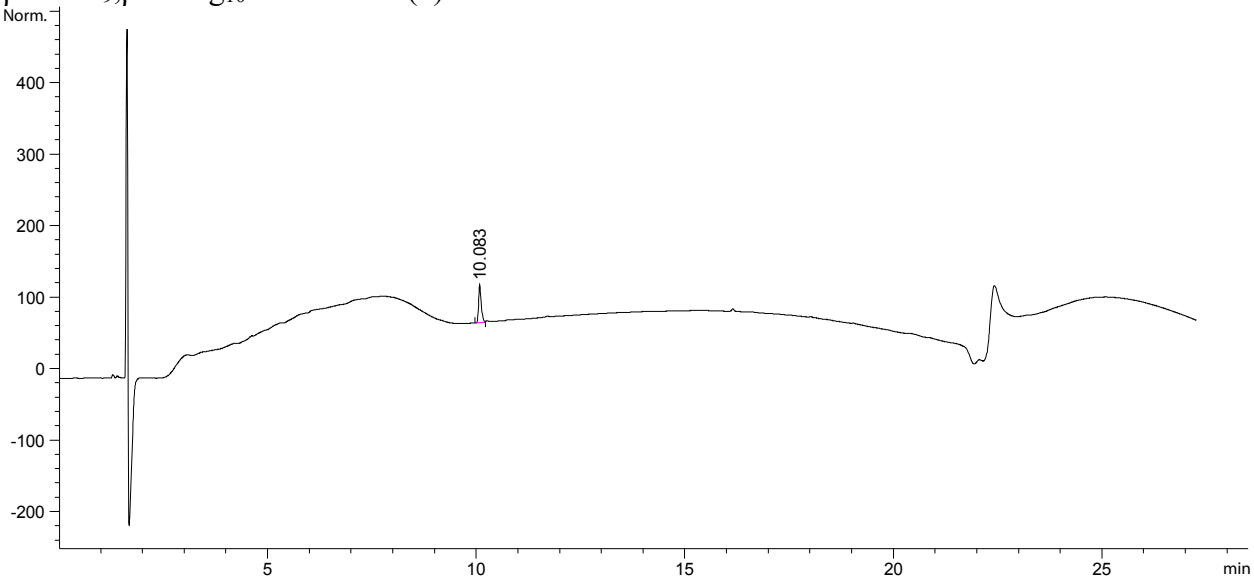

Analytical RP-HPLC was performed on a C18 column with an elution gradient of 5-100% CH_3CN over 20 min.

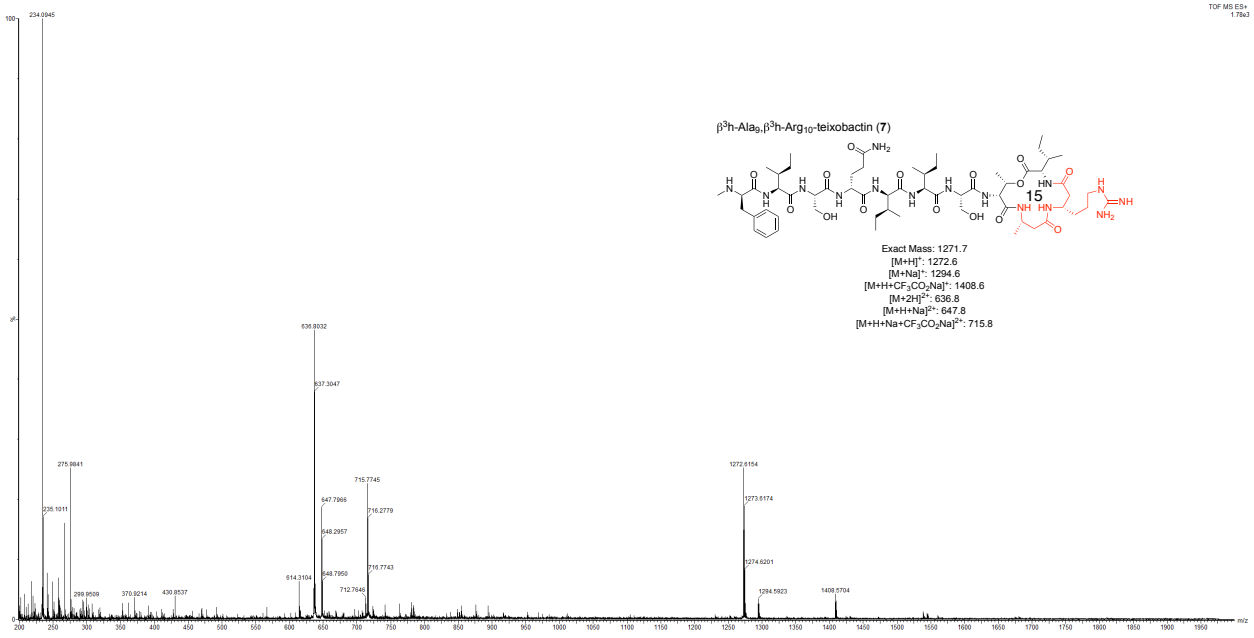

β^3h-Ala$_9$,Arg$_{10}$,β^3h-Ile$_{11}$-teixobactin (**8**)

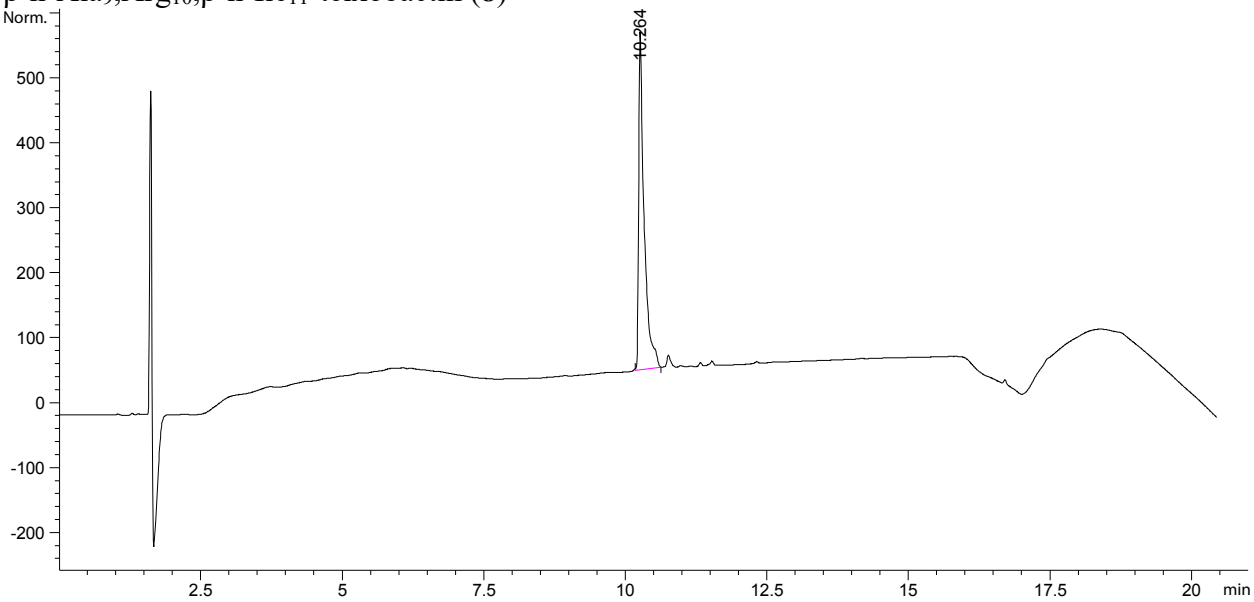

Analytical RP-HPLC was performed on a C18 column with an elution gradient of 5-67% CH_3CN over 15 min.

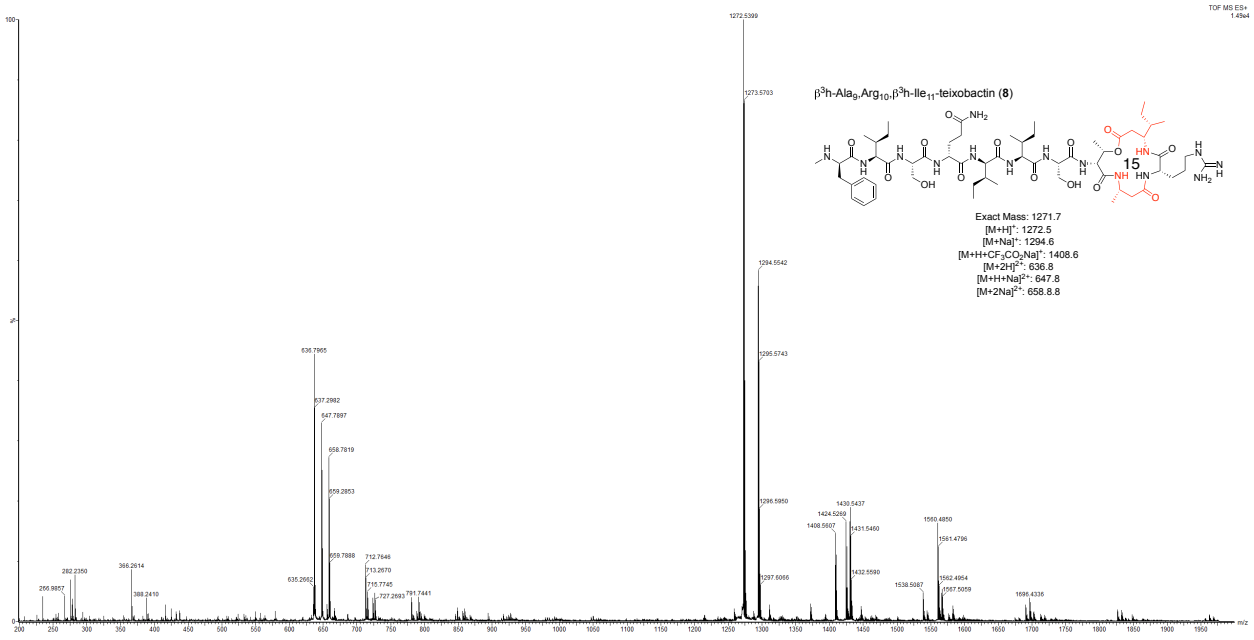

β^3h-Arg$_{10}$,β^3h-Ile$_{11}$-teixobactin (**9**)

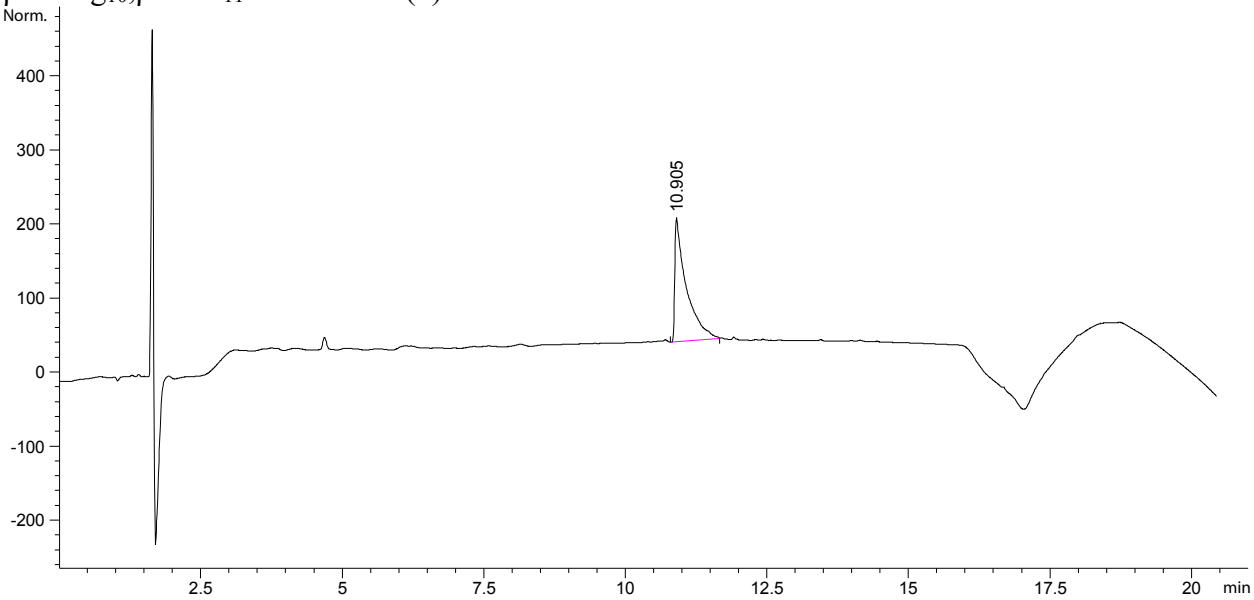

Analytical RP-HPLC was performed on a C18 column with an elution gradient of 5-67% CH_3CN over 15 min.

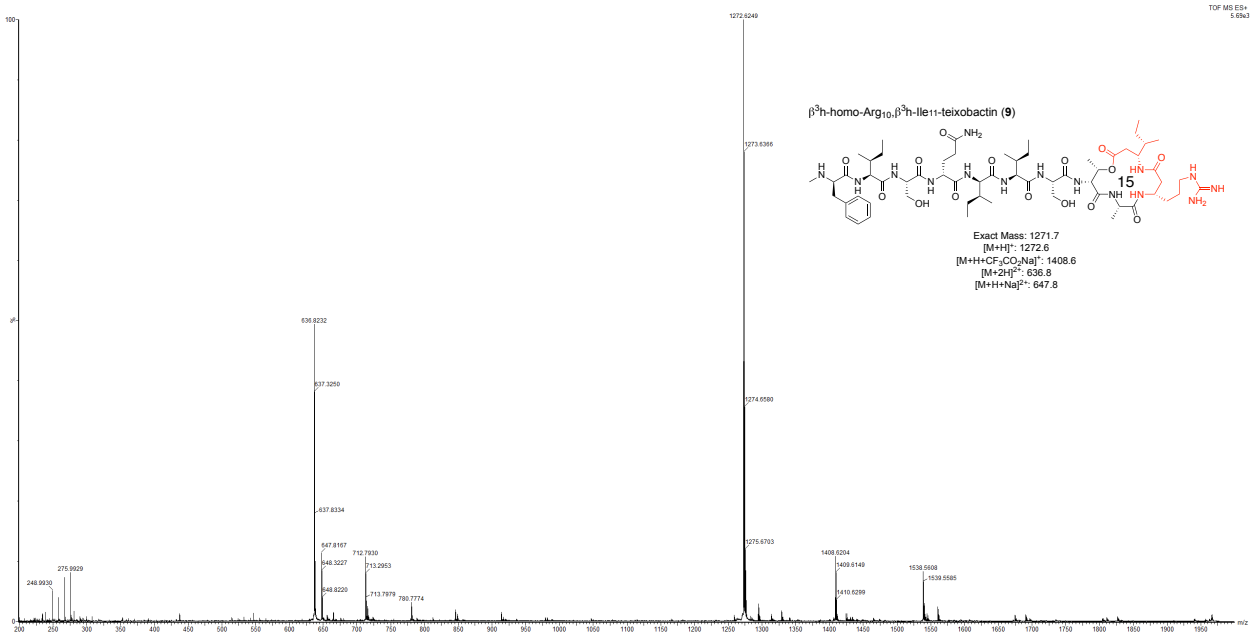

β^3h-Ala$_9$,β^3h-Arg$_{10}$,β^3h-Ile$_{11}$-teixobactin (**10**)

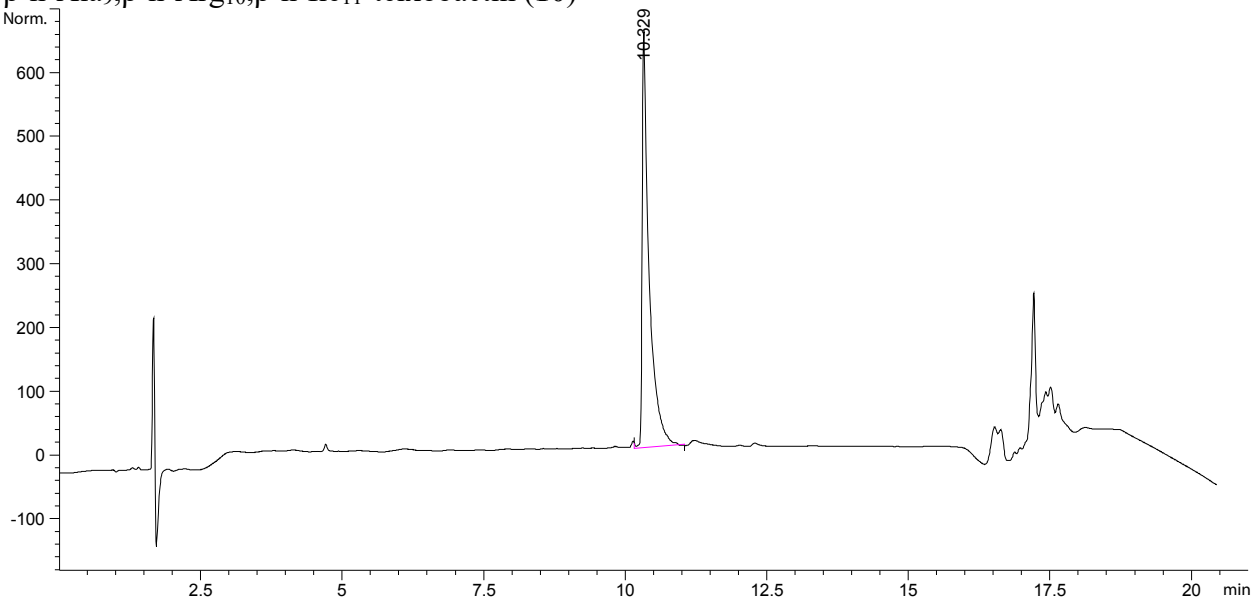

Analytical RP-HPLC was performed on a C18 column with an elution gradient of 5-67% CH_3CN over 15 min.

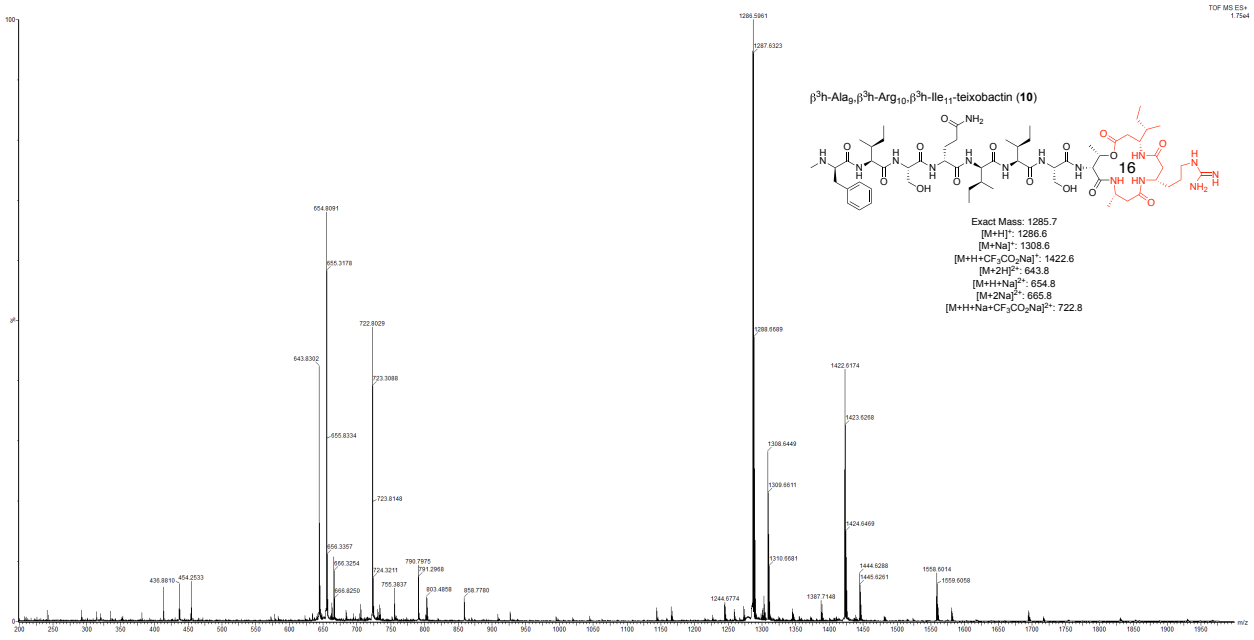

References and Notes

1 The procedure in this section is adapted from and in some cases taken verbatim from Yang, H.; Chen, K. H.; Nowick, J. S. *ACS Chem. Biol.* **2016**, *11*, 1823–1826.

2 Triphenylphosphine-2-carboxamide was synthesized using the procedure reported by Saneyoshi et al. MS (positive ion mode) calcd for $C_{19}H_{17}NOP^+$ $[M+H]^+$ m/z 306.10, found 306.12. [Saneyoshi, H.; Ochikubo, T.; Mashimo, T.; Hatano, K.; Ito, Y.; Abe, H. *Org. Lett.* **2014**, *16*, 30–33.]

3 Chen, K.H.; Le, S. P.; Han, X.; Frias, J. M.; Nowick, J. S. *Chem. Commun.* **2017**, *53*, 11357–11359.

4 The procedure in this section is adapted from and in some cases taken verbatim from Yang, H; Wierzbicki, M.; Du Bois, D. R.; Nowick, J. S. *J. Am. Chem. Soc.* **2018**, *140*, 14028−14032.

5 Kabsch, W. Acta *Crystallogr., Sect. D: Biol. Crystallogr.* **2010**, *66*, 125–132.

6 Foadi, J.; Aller, P.; Alguel, Y.; Cameron, A.; Axford, D.; Owen, R. L.; Armour, W.; Waterman, D. G.; Iwata, S.; Evans, G. *Acta Crystallogr., Sect. D: Biol. Crystallogr.* **2013**, *69*, 1617–1632.

7 Grosse-Kunstleve, R. W.; Adams, P. D. *Acta Crystallogr., Sect. D: Biol. Crystallogr.* **2003**, *59*, 1966–1973.

8 Adams, P. D.; Afonine, P. V.; Bunkoczi, G.; Chen, V. B.; Davis, I. W.; Echols, N.; Headd, J. J.; Hung, L. W.; Kapral, G. J.; Grosse-Kunstleve, R. W.; McCoy, A. J.; Moriarty, N. W.; Oeffner, R.; Read, R. J.; Richardson, D. C.; Richardson, J. S.; Terwilliger, T. C.; Zwart, P. H. *Acta Crystallogr., Sect. D: Biol. Crystallogr.* **2010**, *66*, 213–221.

9 Terwilliger, T. C.; Adams, P. D.; Read, R. J.; McCoy, A. J.; Moriarty, N. W.; Grosse-Kunstleve, R. W.; Afonine, P. V.; Zwart, P. H.; Hung L. W. *Acta Crystallogr., Sect. D: Biol. Crystallogr.* **2009**, *65*, 582–601.

10 Afonine, P. V.; Grosse-Kunstleve, R. W.; Echols, N.; Headd, J. J.; Moriarty, N. W.; Mustyakimov, M.; Terwilliger, T. C.; Urzhumtsev, A.; Zwart, P. H.; Adams. P. *Acta Crystallogr., Sect. D: Biol. Crystallogr.* **2012**, *68*, 352–367.

11 Emsley, P.; Lohkamp, B.; Scott, W. G.; Cowtan, K. *Acta Crystallogr., Sect. D: Biol. Crystallogr.* **2010**, *66*, 486–501.

12 Moriarty, N. W.; Grosse-Kunstleve, R. W.; Adams, P. D. *Acta Crystallogr., Sect. D: Biol. Crystallogr.* **2009**, *65*, 1074–1080.